BEAM DIAGNOSTICS FOR ACCELERATORS

H. Koziol
CERN, Geneva, Switzerland

Abstract
This introductory course aims at a reasonably complete coverage of beam diagnostic devices used in linear and circular accelerators and in primary beam lines. The weight is on the concepts and the indication of variants, while for technical details the reader is referred to the literature.

1. INTRODUCTION

Beam diagnostics is an essential constituent of any accelerator. These systems are our organs of sense that let us perceive what properties a beam has and how it behaves in a machine. Without diagnostics, we would blindly grope around in the dark and the achievement of a beam for physics-use would be a matter of sheer luck (some accelerators have at some time been close to such a situation!). As the saying goes: an accelerator is just as good as its diagnostics.

Beam diagnostics is a rich field. A great variety of physical effects are made use of, imagination and inventiveness find a wide playground. Therefore, there exists today a vast choice of different types of diagnostic devices, each usually in many variants.

Two hours of lecture time do not permit an in-depth coverage of all devices on the market, but to present only a selection would not fulfill the purpose of this course. The choice I have made is to aim for a reasonably complete coverage of diagnostic devices currently used, at the expense of detail. We will thus concentrate on the concepts and indicate the variants that exist and refer to the literature for details.

Also, we will limit ourselves to diagnostics used on accelerators and on ejected primary beams and leave aside detectors for secondary beams, downstream from a target, on their transport to an experimental set-up. As a further economy measure, we will also leave aside associated electronics, analogue signal treatment and digital data treatment, although these are subjects of great importance to beam diagnostics.

There are subjects which have been treated in other lectures, e.g. synchrotron radiation, which permits us to be briefer on those. Very specialized measurements, such as that of beam polarization or those at the final focus of colliding linacs, are beyond the aim of an introductory course and will be just mentioned for completeness.

When setting out to describe a large number of diagnostic devices, one first tries to establish a systematic order. One could proceed according to the properties measured (intensity, position, etc.). Or one could class the devices as electromagnetic, using secondary emission, etc, or as destructive and non-destructive. However, none of that makes much sense. Many devices can measure more than one property, their variants may make use of different physical principles and the distinction between destructive and non-destructive often depends on circumstances.

I have therefore drawn up a matrix (see Table 1) listing the devices to be discussed and the properties they can measure. And now we will forget about classification and get on with the description in a sequence that is didactically convenient.

Table 1

Diagnostic devices and beam properties measured

PROPERTY MEASURED →	Intensity I , Q	transverse: Position	transverse: Size/shape	transverse: Emittance	longit.: Size/shape	longit.: Emittance	Q-value + ΔQ	Energy + ΔE	Polarization	Effect on beam: N	–	+	D
Beam transformers	●				●	●				x			
Wall-current monitors	●	●			●	●				x			
Pick-ups	●	●	(●)		●	●				x			
Faraday cup	●												x
Secondary emission monitors	●	●	●	●				•			x	x	
Wire scanners		●	●	●				•			x		
Wire chamber		●	●								x	x	
Ionization chamber	●										x	x	
Beam loss monitors		•	•	•			•			x			
Gas curtain/jet		●	●	●							x		
Residual gas monitors		●	●	●						x			
Scintillator screens		●	●								x	x	x
Scrapers, targets		●	●	●									x
Schottky scan	●			●		•	●	●		x			
Synchrotron radiation		●	●		●	●				x			
LASER-Compton scattering			●	●					●	x			
Q-measurement							●			x	x		
Emittance measurement				●							x	x	x
Measurement of energy								●		x	x	x	x
Polarimeter									●	x			x

Effect on beam : N none
– slight, negligible
\+ perturbing
D destructive

Only the most basic measured properties are shown. There are many more, less basic,which can be derived: coupling, dispersion, chromaticity, etc.
Note that to determine emittance (transverse or longitudinal), knowledge other than that obtained from the basic measurement is required.
The oscillatory behaviour of the beam is observed through the time-dependance of properties (like position, size/shape, energy), often on a very fast time scale.

2. DESCRIPTION OF DIAGNOSTIC DEVICES

2.1 Beam transformers

Apart from the sheer proof of its existence, the most basic measurement on a beam is that of its intensity. A widely used device is the "beam transformer" (an older name, Rogowski coil, is still sometimes used) which allows one to determine the electric current that a beam constitutes or, depending on the circumstances, the electric charge contained in a burst of beam [1,2]. Figure 1 shows the principle.

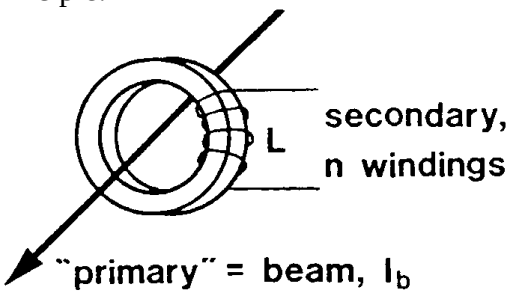

Fig. 1 Principle of the beam transformer.

In order for the transformer to see the magnetic field produced by the beam, it must be mounted over a ceramic insert in the metallic vacuum chamber. The ferromagnetic core is wound of high-permeability metal tape or made of ferrite, to avoid eddy currents. Bandwidths exceeding 100 MHz can thus be achieved. An idealized transformer with a secondary winding of inductance L and connected to an infinite impedance would deliver as signal a voltage

$$V = L\frac{dI_b}{dt}$$

which, as Fig. 2 shows, is "differentiated" and not very practical to use.

In reality, the ferromagnetic core has losses proportional to f^2 (f = frequency), the secondary has a stray capacity C_s and is terminated with a finite resistance R (Fig. 3).

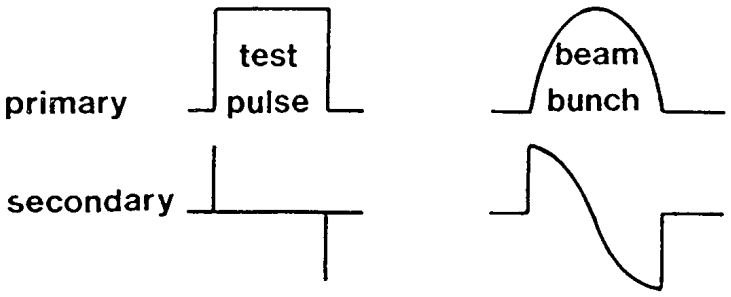

Fig. 2 Signal from an idealized transformer into an infinite impedance.

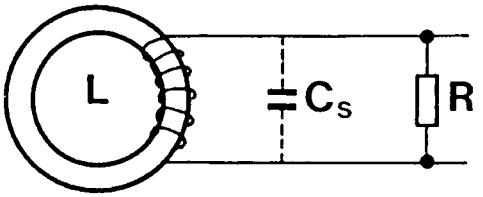

Fig. 3 Real beam transformer with stray capacity C_s and termination R.

The signal now shows a much more useful behaviour (Fig. 4). Provided the length of a beam bunch is longer than the transformer's rise time and shorter than its droop time, the signal will be a good reproduction of the bunch shape.

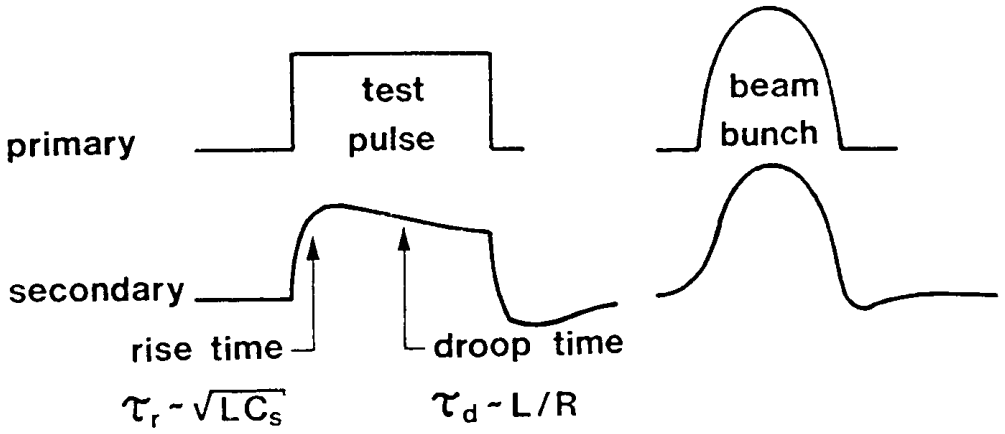

Fig. 4 Signal from real transformer.

When instead of a single bunch a long string of bunches passes through the transformer, as is also the case with a circulating beam, the droop will affect the base line (Fig. 5). When equilibrium has been reached, equal areas of signal will be above and below zero. Thus, the level of the base line is a measure for the dc component of the beam current.

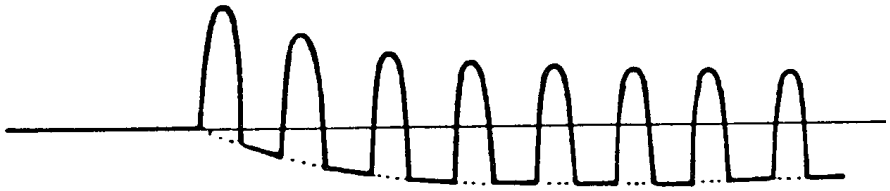

Fig. 5 Droop of base line in the transformer signal.

For a beam circulating in a machine, the succession of bunches seen by the transformer will be much longer than its droop time. Therefore, to obtain a signal representing the beam intensity, one has to electronically treat the transformer's signal such that the effective droop time is much longer than the time that the beam circulates. At the same time, this increases the signal rise time, so that the bunch structure will disappear. Such a treatment is often called a "low pass" or "integration". Figure 6 shows three commonly used methods.

Since integration makes the bunch structure disappear anyway, it will also produce an intensity signal for an unbunched beam, without any longitudinal density structure, provided that signal observation begins before injection of the beam.

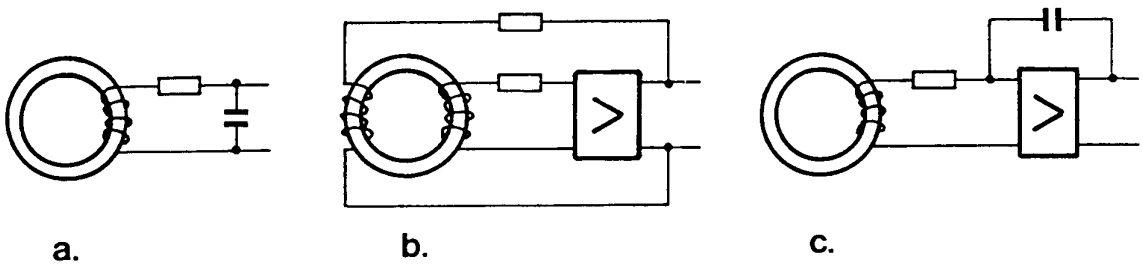

Fig. 6 Integration of signal from a beam transformer.

a) Simple RC circuit. b) Inductive feedback (Hereward transformer).
c) Capacitive feedback (Miller integrator).

Adding a simple RC may sometimes suffice, but in general, the time constants will be too short and/or the signal too attenuated. Feedback integrators [1,2] allow time constants above 1000 s to be achieved, while maintaining good signal level. They are widely used on circular accelerators, where cycle times are of the order of seconds.

In a storage ring, however, the beam may circulate for hours. Indeed, 999 h, or 42 days, is the longest a beam has circulated uninterrupted (in the Antiproton Accumulator at CERN). No integrator can cope with that, a true dc beam current measurement is needed. Such a device [3,4] was developed for the ISR (the CERN Intersecting Storage Rings), the first machine to sustain beams for hours. Figure 7 shows its principle.

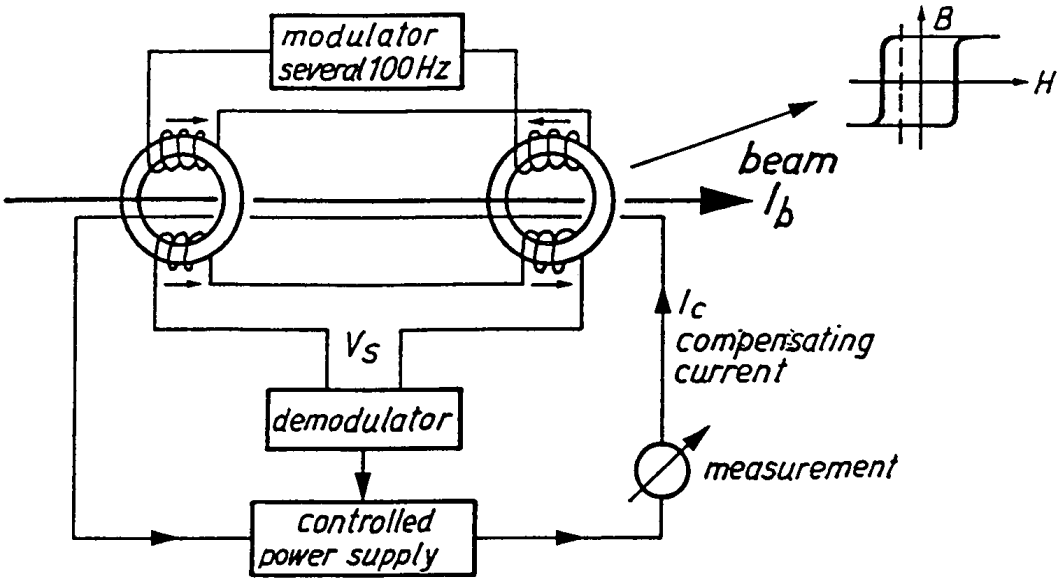

Fig. 7 Basic scheme of a dc beam transformer and rectangular hysteresis of core material.

A modulator sends a current at several 100 Hz through the excitation coils of two ferromagnetic rings, such that they are excited in opposite directions. The pick-up coils mounted on the rings are connected in series, their sum signal, V_S, will thus be zero. The rings are made of a material with rectangular hysteresis. When a beam current I_b passes through the rings, it introduces a bias in the excitation of the cores, V_S will no longer be zero and the second harmonic of the modulator frequency will appear in it, which the demodulator converts into a dc voltage. This controls a power supply, sending a current I_c through a compensating winding on the two rings. Equilibrium is reached when the compensating current I_c cancels the beam current I_b. The final measurement is that of I_c. Proton currents of over 50 A have been measured with such a dc beam transformer, a resolution of better than 1 μA has been achieved and the zero drift over a week is of the same order.

Such dc beam transformers have become commercially available, for various ranges of current and sensitivity.

2.2 Wall-current monitors

One may want to observe the bunch shape at frequencies far beyond the few 100 MHz accessible with beam transformers. The bunches may be very short, as is often the case with electrons or positrons, or they may have a structure in their line density, caused by intentional processes or by instabilities.

Wall-current monitors with a bandwidth of several GHz have been built [5,6,74,75]. Their principle is quite simple (Fig. 8a) :

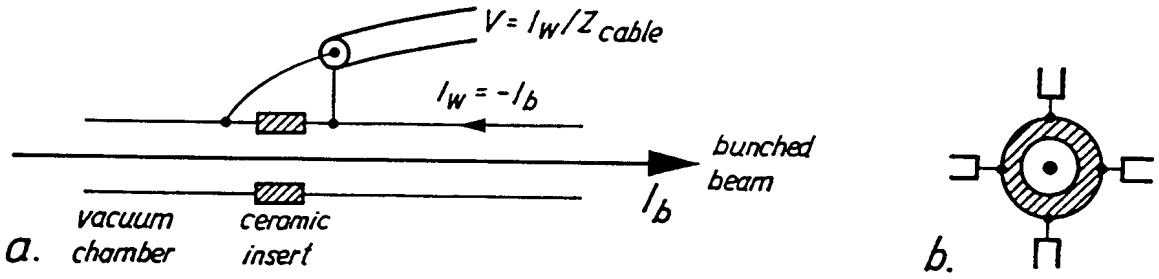

Fig. 8 a) Principle of wall-current monitor. b) Separate pick-up of signals to observe beam position.

A modulated beam current I_b is accompanied by a "wall current", I_W, which it induces in the vacuum chamber, of equal magnitude and opposite direction. An insulating gap forces the wall current to pass through the impedance of a coaxial cable. The gap may also be bridged with resistors, across which a voltage is picked up. To avoid perturbation through circumferential modes, the wall current (or the gap voltage) is picked up at several points around the circumference and summed. When the beam is not at the centre of the vacuum chamber, the wall current will be unequally distributed around the circumference of the chamber. Separate pick-up and separate observation (Fig. 8b) [6] will thus also show the beam position with GHz bandwidth.

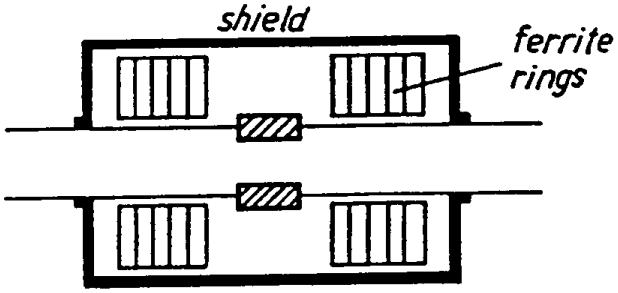

Fig. 9 Gap of wall-current monitor with shield and ferrite loading.

A conducting shield must be placed around a wall-current monitor. Without it, troublesome electromagnetic radiation from the beam would leak out through the gap and the monitor itself would be perturbed from the outside. Of course, the shield constitutes a short-circuit at low frequencies and thus severely limits the lower end of the monitor's bandwidth. Loading the volume of the shield with ferrite increases the inductance and the cut-off can be lowered to some 100 kHz, sufficient for undifferentiated observation of bunch shape in most accelerators.

2.3 Position pick-up monitors (PU)

The measurement of transverse beam position is a field of particularly great diversity. A glance at Table 1 shows a host of detectors, based on various physical effects. The ones treated in this chapter are of three kinds (see [75] for an excellent tutorial overview) :

- electrostatic,
- magnetic,
- electromagnetic.

Widely used, in particular on circular accelerators with not too short bunches, is the electrostatic PU [7, 8, 9, 10]. In its simplest form it resembles a diagonally cut shoe-box (Fig. 10 a, b). A combination of a horizontal and a vertical PU is shown in Fig. 11.

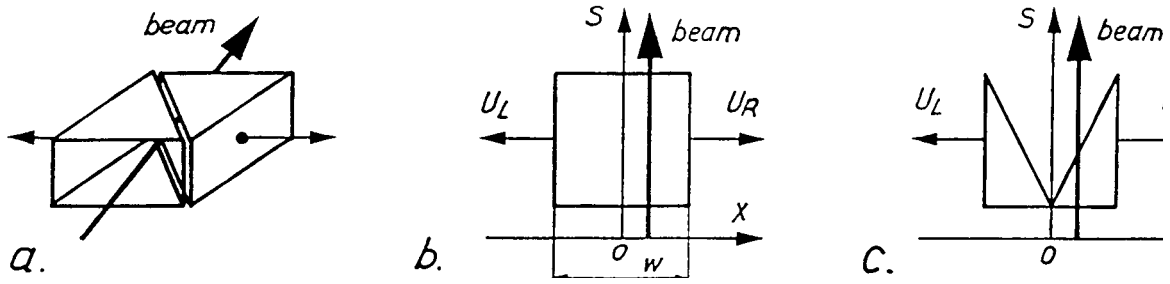

Fig. 10 a) Diagonally cut "shoe-box" PU. b) Basic geometry and tapping of signals.
c) A variant which allows interleaving of a horizontal and a vertical PU.

As it passes through, the beam will induce electric charges on the metallic electrodes, more on the one to which it is closer, less on the other, but their sum remaining constant, independent of beam position. The induced charges can be carried away for measurement into a low-impedance circuit or be sensed on a high impedance as a voltage on the capacity between the electrode and the surrounding vacuum chamber. The effect being linear, the position of the beam with respect to the PU centre is readily derived :

$$x = \frac{w}{2} \frac{U_R - U_L}{U_R + U_L}$$

Frequently, the jargon terms "Δ" and "Σ" are used : $\Delta = U_R - U_L$ and $\Sigma = U_R + U_L$. Using them :

$$x = \frac{w}{2} \frac{\Delta}{\Sigma}$$

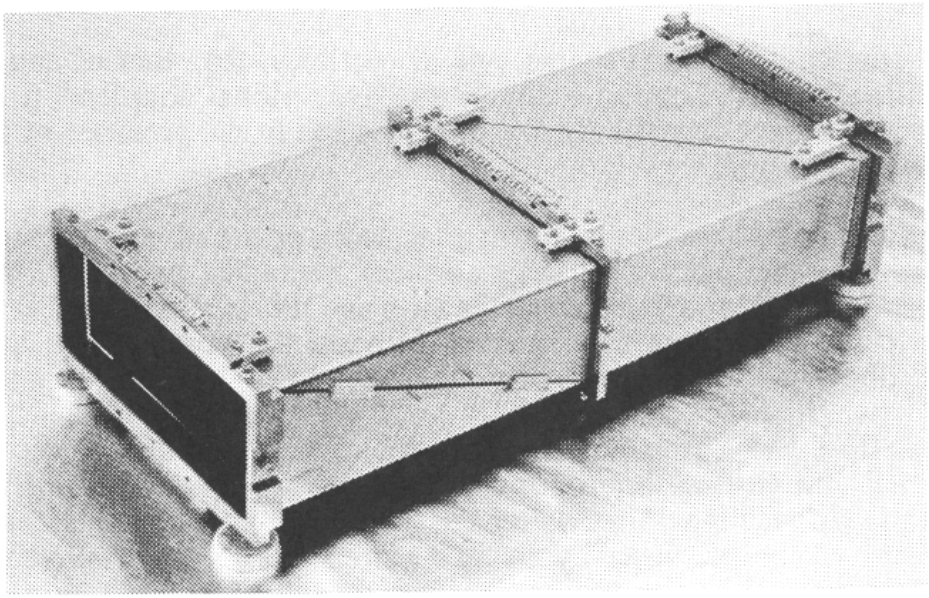

Fig. 11 Combination of a horizontal and a vertical PU, mounted in the vacuum chamber of the Antiproton Accumulator at CERN.

The linear relation holds for any shape of the electrodes as long as, projected onto the plane in which the position is measured, the length of the electrodes is a linear function of the distance from the axis. The shape of the electrodes may thus be deformed to suit practical

requirements [11]. A variation is shown in Fig. 10c, where the gap left free allows the placement of two further electrodes for the orthogonal plane. However, although $U_R - U_L$ still depends linearly on beam position, $U_R + U_L$ is no longer independent of it. For normalization, the sum of all four electrodes must be used.

Edge effects at the ends of the electrodes may impair the linearity [12]. To avoid them, one either designs the electrodes to have the same cross-section as the vacuum chamber to either end of them, or one provides cross-sectional continuity by adding guard electrodes at both ends.

In electron and positron machines, no electrodes can be tolerated in the mid-plane : there they would be hit by the synchrotron radiation and the resulting secondary electron emission would perturb the signal. So-called "button" electrodes [13, 14, 15, 76] are used, housed in recesses (Fig. 12a).

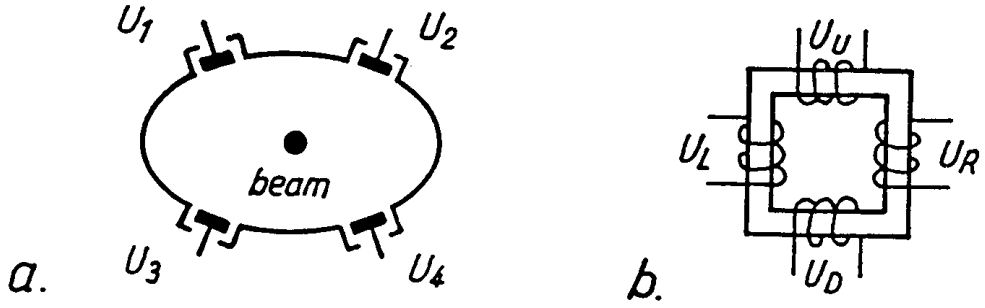

Fig. 12 a) PU with "button" electrodes. b) Magnetic PU.

Compared with the shoe-box PU, for the measurement of horizontal position $U_1 + U_3$ replaces U_L , and $U_2 + U_4$ replaces U_R, similarly for the vertical plane. The response to position is not linear and the two planes are interdependent. Careful calibration and consequent data treatment on the signals is necessary.

In proton machines too, secondary emission from the electrodes can be a problem when strong beam loss occurs. In such a situation, a magnetic PU [16] may be chosen (Fig. 12b).

In single-ring colliders, two beams, one of particles, the other of anti-particles, are circulating simultaneously, in opposite directions. "Directional couplers" [17, 18, 19, 20] permit the selective observation of only one of the beams in the presence of the other. The principle is shown in Fig. 13a.

The beam acts in two ways on the strip electrodes of the coupler. Firstly, the electric charge of the passing beam induces a charge on them. Secondly, part of the magnetic field, created by the beam current, passes between the strip and the vacuum chamber and induces a voltage. These two effects add for the direction of the beam shown in Fig. 13a, and cancel for a beam of opposite direction.

Four strips (Fig. 13 b), after suitable formation of sums and differences of the signals, give the horizontal and vertical beam position. The sensitivity of such a PU depends on frequency as (sin f) with the maximum where the strip length corresponds to a quarter wave length. The response can be influenced by giving the strips more sophisticated shapes [18].

A "wave-guide coupler" (Fig. 14), [21] can be used, usually on electron and positron linacs, to observe extremely short bunches (<< 1 nsec). The beam passing through it sets off a wave which propagates to the left and the right where it is picked up by small loops on the inside of the wave guide. The position is not derived by comparing the magnitude of U_L and U_R, but by comparing their phase : $x \sim \Delta\varphi$

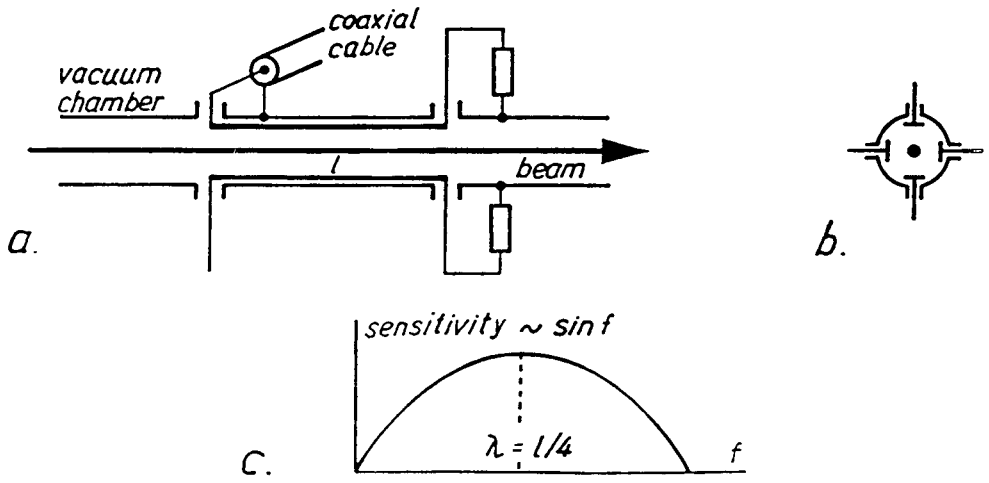

Fig. 13 a) Principle of directional coupler. b) Cross-section with four coupler strips. c) Frequency response.

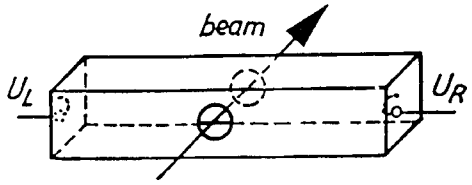

Fig. 14 Wave-guide coupler. Beam position affects the right/left path-lengths of the induced wave, resulting in a phase difference between U_L and U_R .

To measure the closed orbit in a circular accelerator, many PUs are arranged around the circumference. A rule-of-thumb says that at least four position measurements per betatron wavelength are required to see closed orbit distortions sufficiently well. E.g. a Q-value around 3.5 demands at least 14 PUs, uniformly spaced not in linear length but in betatron phase advance. From that minimum one will then go up to the nearest number that fits with the periodicity of the machine for a regular pattern of installation.

Special kinds of PU have been conceived to obtain information on the shape of the beam [22, 23, 24], in terms of aspect ratio between its horizontal and vertical size. This is a very tricky task and quantitatively satisfactory results are difficult to obtain.

2.4 Faraday cup

Conceptually the simplest way to measure beam current is to capture the beam and let the current flow through some kind of meter. Historically, this was also the first method used. It is still employed at low energies, where the obvious condition of the thickness of the collector plate being greater than the stopping range of the beam particles can be easily fulfilled. Here are some ranges for protons in copper :

500 keV	pre-accelerator : Cockcroft-Walton or RFQ	0.003 mm
5 MeV	van de Graaff generator	0.08 mm
50 MeV	injector linac	4 mm
200 MeV	injector linac	43 mm
1 GeV	small synchrotron	520 mm

Capture of the beam with a simple collector plate suffers from perturbation through secondary electron emission. Electrons liberated from the collector surface escape into the surroundings, thereby contributing in an uncontrolled way to the current flowing through the meter. The use of a Faraday cup (Fig. 15) prevents this from happening. The collector is

housed in a box with a hole to let the beam in and at a negative potential of a few 100 V to drive the secondary electrons back onto the collector.

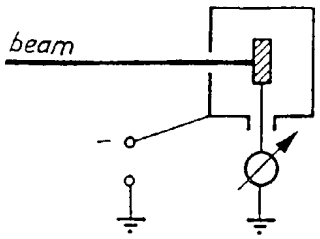

Fig. 15 Faraday cup.

2.5 Secondary-emission monitors (SEM)

At this point, the reading of Appendices 1 and 2 is recommended. They cover some features common to the detectors described in this and several following sections.

A SEM makes use of the phenomenon that under the impact of the beam particles on some solid material electrons are liberated from the surface, thus producing a flow of current.

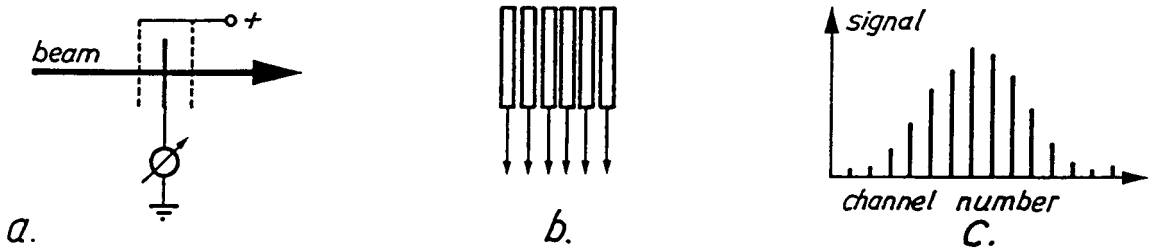

Fig. 16 a) Basic SEM : foil with clearing electrodes, seen sideways. b) A SEM consisting of an array of ribbons , seen in beam direction. c) Transverse beam profile obtained from an array of ribbons or wires.

When the intercepting material is a foil (Fig. 16 a), electrons are liberated from both sides. Since this is a surface phenomenon, the secondary emission coefficient will not only depend on the material but also, often even critically, on the state of cleanliness of its surface.

The provision of a "clearing field" of a few 100 V/cm is essential to ensure that the liberated electrons are rapidly cleared away. Otherwise, an electron cloud may form over the foil surface and impede further emission.

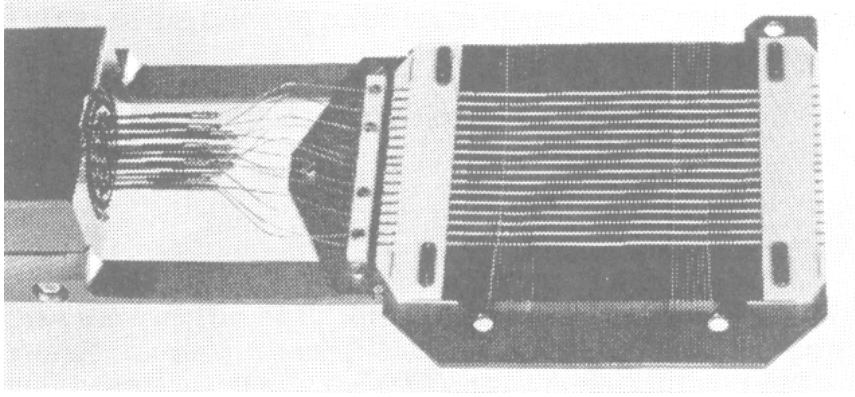

Fig. 17 A SEM made of thin ribbons attached to contacts on a ceramic frame.

A SEM in the form of an array of thin ribbons (Figs. 16b and 17) is a much-used device to measure transverse density distribution [25]. Sequential display of the signals from the ribbons gives the beam profile (Fig. 16c). To enhance the signal strength, either the individual ribbons or the whole array may be inclined with respect to the beam direction, thus presenting a greater effective surface. When signal strength is not a problem, the array and the clearing electrodes may be made of thin wires. This makes it a nearly non-destructive profile monitor (at least for single passage, not for a circulating beam).

2.6 Wire scanners

When a SEM, made of several wires, disturbs the beam too much, mostly through multiple Coulomb scattering, a single wire may be moved across the beam. This can be done in steps and a reading is taken, e.g., at every pulse of a linac.

A fast moving wire can be used even on a circulating beam [26, 27, 28, 29]. Speeds of 20 m/s have been obtained with a 50 μm diameter Be wire, which allowed profiles to be measured on an 800 MeV proton beam with acceptably small emittance increase (Fig. 18).

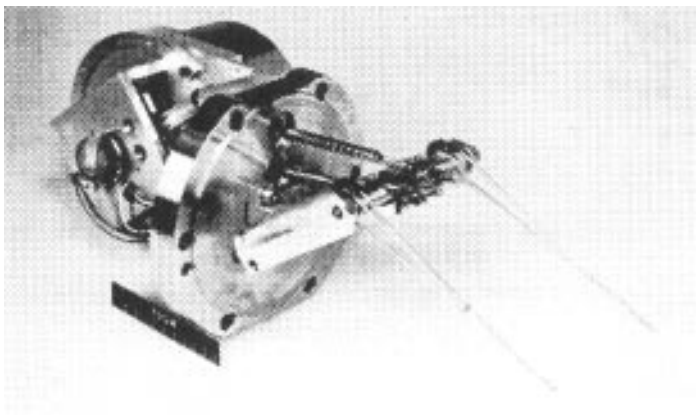

Fig. 18 Fast wire scanner. The wire, extended between the tips of the lightweight arms, is only 50 μm in diameter and thus barely visible.

Wire scanners too need a clearing field in order to obtain a consistent signal. The clearing electrode will be situated well outside the beam cross-section.

An alternative is not to use the secondary emission current at all but to place radiation detectors at the outside of the vacuum tank in which the wire moves and look at the products of the collisions between beam particles and wire material (γ and secondary particles). This may require thin parts in the wall of the tank, and the signal from two or more radiation detectors to be summed to render the sensitivity independent of wire position.

2.7 Multi-wire chambers

These detectors, taken over from high energy physics [30], find some application on beams of very low intensity. At LEAR (the CERN Low Energy Antiproton Ring) for example, by means of an "ultra-slow extraction", on average as little as one antiproton can be ejected per revolution, yielding beams of less than 10^6 π/s.

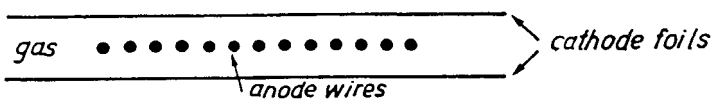

Fig. 19 Multi-wire chamber. Typically, the distance between the cathode foils is 10 mm, t he distance between wires 1 mm, their diameter 5 to 50 mm and their potential + 5 kV.

Electrons produced in the gas by the passing beam particles will travel towards the nearest wire. In the high gradient close to the wire they experience strong acceleration and create an avalanche. A wire chamber can be used in counting or in proportional mode. The distribution of counting rate or signal height over the wires represents the beam profile.

2.8 Ionization chamber

This is a gas-filled, thin-walled chamber with a collector electrode inside. Particles passing through it will ionize the gas, the ions will travel towards the cathode, the electrons towards the anode and a current can be measured (Fig. 20). The voltage should be in the "plateau" region where all charges are collected but no avalanche occurs.

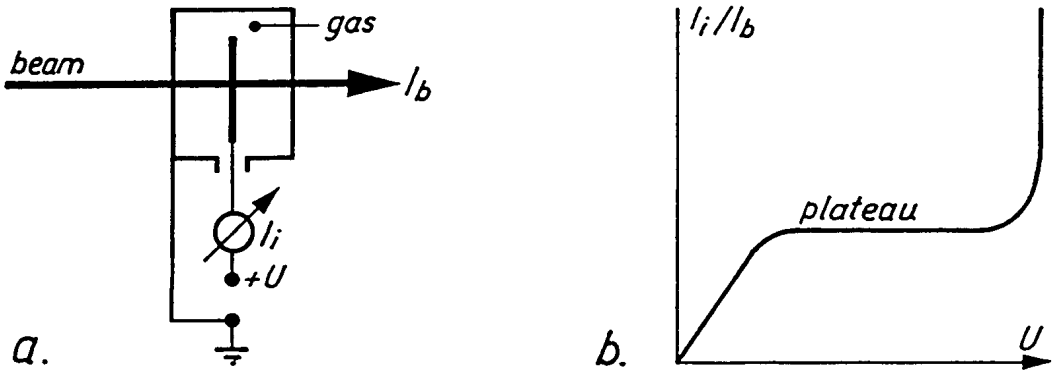

Fig. 20 a) Ionization chamber. b) Collection efficiency vs. voltage.

Ionization chambers are used to measure very low beam intensities and as beam loss detectors (see section 2.9).

2.9 Beam loss monitors (BLM)

Although they do not measure a beam property, the information which they supply is most valuable for the practical operation, in particular of high intensity machines, where the loss of a minute fraction of the beam, too small to be reliably measured with beam transformers, causes intolerable levels of radiation and/or induced radioactivity of components. High intensity machines are therefore equipped with a large number of BLMs around their circumference to indicate the location and magnitude of losses for remedial action, sometimes in a fast, automatic way.

On accelerators employing superconducting magnets, the heat deposited in the superconductors by the loss of even minute fractions of the beam can cause a "quench", that is the loss of superconductivity of a part of the magnet coil, with potentially disastrous consequences. There, BLMs are indispensible elements in the safety chains which dump the beam in a safe way before the losses can rise to dangerous levels.

Calibration in terms of number of particles lost is usually obtained by intentional loss of a measured fraction of the beam but is neither easy nor very precise. Besides the pure statement of loss, BLMs with a fast response yield information on its cause and mechanism.

Three widely used kinds of BLM will be briefly described :

- Ionization chamber (see section 2.8),
- Aluminium Cathode Electron Multiplier (ACEM),
- Scintillator plus photomultiplier (PM).

An ACEM [31, 32] is similar to a PM, with a thin aluminium layer on the inside of the glass tube serving as the cathode. Electrons are produced from the cathode through secondary emission when it is struck by a stray beam particle, a γ-ray, or some secondary particle resulting from beam loss. As with a PM, the gain is high and adjustable over a wide range and an ACEM is cheap, robust and radiation resistant.

A further very cheap and effective BLM is a combination of a scintillator and a PM as shown in Fig. 21, [33]. The primary effect here is the production of light.

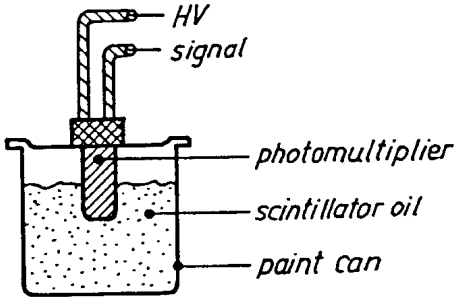

Fig. 21 A photomultiplier immersed in scintillator oil is a cheap and fast beam loss monitor.

With this type, bandwidths of 100 MHz are possible, allowing one to see details such as loss from only part of the bunch length, as happens, e.g., when a kicker magnet is incorrectly triggered.

2.10 Gas curtain or jet

In section 2.6 we have seen that a fast wire scanner is a means to measure the transverse profile of a beam circulating in an accelerator, once or twice per cycle. In a storage ring, where one wants to measure the profile repeatedly over the many hours that a beam circulates, a wire scanner would cause too much scattering and emittance increase. Only a gas constitutes an even more transparent interceptor. Figure 22 shows the gas curtain [34] developed for the ISR.

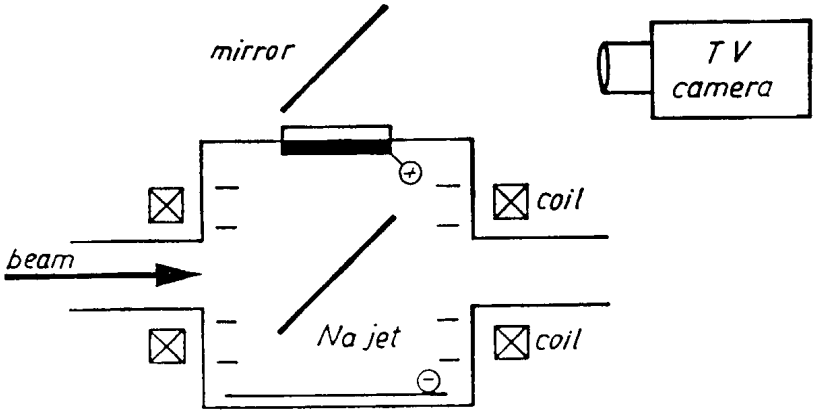

Fig. 22 Sodium-curtain beam profile monitor, seen in the direction of the Na-jet.

An ultrasonic 2-dimensional jet of atomic Na is produced in an oven followed by a collimation system. The Na-jet is inclined at 45° to the beam direction. Electrons from the ionization of Na atoms by beam particles are accelerated by a vertical electric field, while being focused along the lines of a magnetic field, also of vertical direction. On the top of the tank there is a quartz window which on the inner side carries a layer of scintillator (incorrectly often called phosphor), covered with a very thin metal layer as anode for the electric field. The accelerated electrons will traverse the metallization and produce light in the scintillator, thus

forming a 2-dimensional image of the beam cross-section. This image can be viewed with an image-intensifier TV camera for direct display or with some other device for further data treatment.

All this sounds easy but in practice is very difficult to realize because of the stringent boundary conditions. The magnetic field needs to be compensated by additional coils on either side of the detector, so as not to perturb the closed orbit. The Na-jet must be extremely well collimated and entirely collected on the other side to avoid contamination of the vacuum. Its density must be controlled to constitute only a small increase in the average pressure of the ring. Consider the circumference of the ISR of 1 km and an average pressure of 10^{-11} Torr. A Na-curtain 1 mm thick and of an equivalent pressure of 10^{-5} Torr will double the average pressure around the circumference!

The ISR have been dismantled and the Na-curtain monitor with them. It will probably remain the only one of its kind, but many lessons have been learnt from its design and operation.

That a gas curtain must not increase significantly the average pressure around the ring is a condition even more difficult to fulfill on a small machine like LEAR, with only 80m circumference and a vacuum in the 10^{-12} Torr range. But some such device is needed there to observe the fast changes in beam emittance under the action of electron cooling. The solution is to pulse the gas jet only for a brief interval, when a measurement is made. A pulsed atomic carbon jet of a few 100 μsec duration is produced by directing a strong pulsed LASER beam onto a carbon target [35]. Otherwise, the device is similar to the one described for the ISR.

2.11 Residual-gas monitors

When neither the residual gas pressure nor the beam intensity are too low, ionization of the "natural" residual gas may supply electrons in sufficient number and a gas curtain is not needed. The image appearing on the scintillator will however not be 2-dimensional, it is the projection of the beam density distribution onto one plane. Two devices are needed for a horizontal and a vertical profile [77,78,79].

The Ionization Beam Scanner (IBS) [36] is a further device relying on residual gas. It employs a time-varying electric and a static magnetic field, at right angles to each other and to the beam, to guide the ionization electrons towards a collector or electron multiplier. Although a precise instrument for low intensity beams, the IBS is too easily perturbed by the space-charge fields of intense beams.

Instead of collecting electrons from the ionization, one can also observe the light from de-excitation of the residual gas atoms [37]. This is achieved more easily at the low energies of a pre-injector (500-800 keV) combined with the prevalent modest vacuum.

2.12 Scintillator screens

Scintillators were the first particle detectors, a century ago. When accelerators, instead of cosmic radiation and radioactive samples, began to deliver particles, scintillators were the prime means to detect the existence of a beam and its location. Although many people turn up their nose at them as an old-fashioned relic from pioneer days, scintillator screens are still alive and not beaten in their simplicity, cheapness and power of conviction. Even today, where everything gets digitized, data treated, fitted, smoothed, enhanced and finally displayed (or perhaps just because of that?), there is nothing as convincing as a flash of light, dead on the centre of a scintillator screen.

After that philosophical excursion, back to technical matters. Fig. 23 shows a typical arrangement for measuring beam position and, less quantitatively, size. A scintillator screen (sometimes incorrectly called phosphorescent or luminescent) is moved into the path of the beam. It is inclined at 45° to the beam, carries a graticule and is illuminated through a small window in the tank. Through another window, at 90° to the beam direction, a TV camera will see a 2-dimensional image of the beam cross-section. Figure 24 shows a vertically moved screen in its tank.

The most common scintillator used to be ZnS powder which, with some binder, was painted onto a metal plate. Such screens deliver green light and have high efficiency but are unfit for use in high vacuum and are burnt out at some 10^{14} protons/cm^2 at GeV energies.

A great step forward was the formation of thick Al_20_3 layers on aluminium plates under simultaneous doping with Cr [38]. Chemically, this is the same as ruby and the light emitted is red. These screens are fit for ultra high vacuum and have a long lifetime (10^{20} to 10^{21} p/cm^2 at 50 MeV). Recent use is described in Ref. [39].

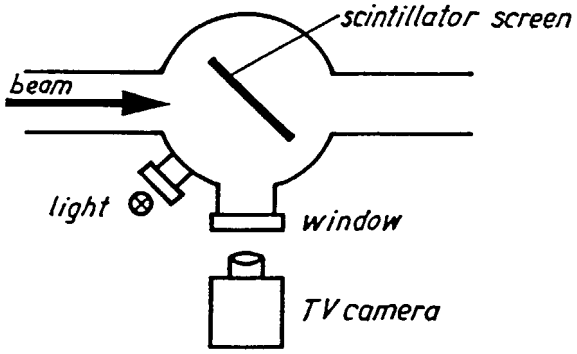

Fig. 23 Typical arrangement for observation of beam position and size with a movable scintillator screen and a TV camera.

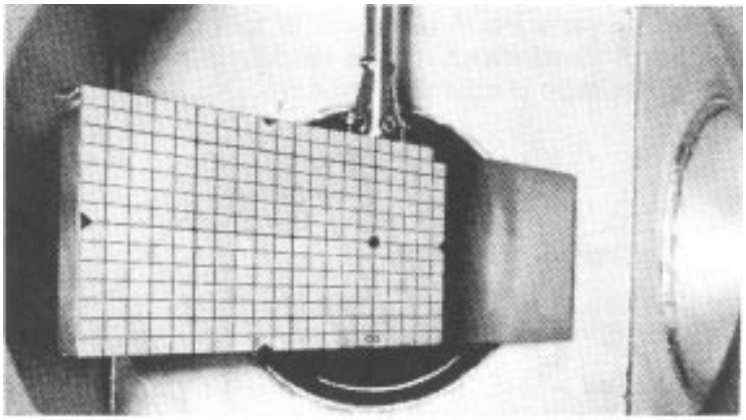

Fig. 24 Scintillator screen made from a Cr-doped Al_20_3 plate with imprinted graticule.

At CERN, the most-used screens are now thin plates (1 mm or less) of Cr-doped Al_20_3 which can be obtained from industry in all sizes with a graticule and other references printed directly on their surface [80]. The screen shown in Fig. 24 is of that kind and Fig. 25 shows another one, mounted on the antiproton production target of the Antiproton Accumulator. It has received some 10^7 pulses of 10^{13} protons at 26 GeV in a spot of about 3 mm diameter (every 2.4 s during some 6000 h of operation in 1 year), i.e. over 10^{20} p/cm^2. This was and still is the most important means of keeping the beam on the target with a precision of ± 0.5 mm.

Several aspects of the TV camera deserve attention. Often it needs to be radiation resistant. The model developed at CERN uses nuvistors and stands 10^8 Rad. Ordinary lenses

turn brown under radiation. Catadioptric optics do a bit better but when radiation is really a problem, one has to buy expensive lenses developed for use in reactors.

For very weak beams a combination image intensifier - Vidicon is used. Beams of 10^9 protons of GeV-energy in a cross-section of a few cm^2 are clearly visible. Also, CCD-cameras offer high sensitivity, but are little resistant to radiation.

TV images may be digitized and stored, for more convenient observation or image treatment to extract more quantitative information.

Fig. 25 Scintillator plate mounted on the antiproton production target of the CERN Antiproton Accumulator.

2.13 Scrapers and measurement targets

Incremental destruction of a beam with scrapers permits the determination of the betatron amplitude distribution of the particles. A scraper with four movable blades (Fig. 26), used in conjunction with a dc beam transformer, allows measurement in the horizontal and vertical plane in a storage ring, where there is time to move the blades towards and into the beam.

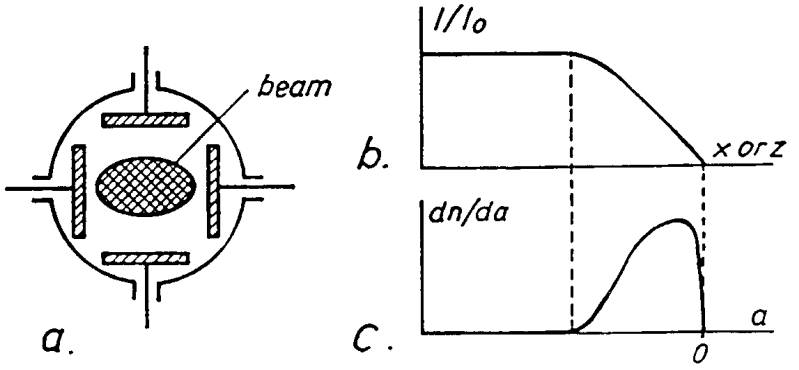

Fig. 26 a) Scraper with four blades for horizontal and vertical measurement.
b) Beam intensity vs. blade position. c) Amplitude distribution.

Observing the decrease of beam intensity as a blade advances, one obtains the beam size for a given fraction of the total intensity and, through differentiation, the amplitude distribution. In principle, a single blade in each plane would suffice, but for independent and consistent determination of the beam centre, two, one on each side, are needed. In the horizontal plane, the distribution of the particles is given by the spread in betatron amplitude and by the spread in momentum. Either one places the scraper where the dispersion is zero or one has to unfold the two spreads.

Although scrapers are destructive and slow, they are valuable for their precise and reliable information. They can serve for the calibration of non-destructive emittance measurements, such as Schottky scans of betatron bands (see section 2.14) and for intentional limitation of machine acceptance.

The beam particles are not stopped in the scraper blades, they are merely scattered. After several traversals of the blades their betatron amplitude has grown beyond the machine acceptance and they are lost somewhere around the ring. Energy loss in the blades usually plays a lesser rôle.

On accelerators with their short cycle time and fast-shrinking beam size, scrapers as described above are not applicable. The same principle can still be employed by driving the beam into a stationary blade by means of a pulsed closed orbit distortion [40]. Fast measurement targets have also been built (Fig. 27). The position of the two blades is pre-adjusted and then the target is flipped into the beam in a movement perpendicular to the plane of measurement. Interception times of only a few ms are thus achieved.

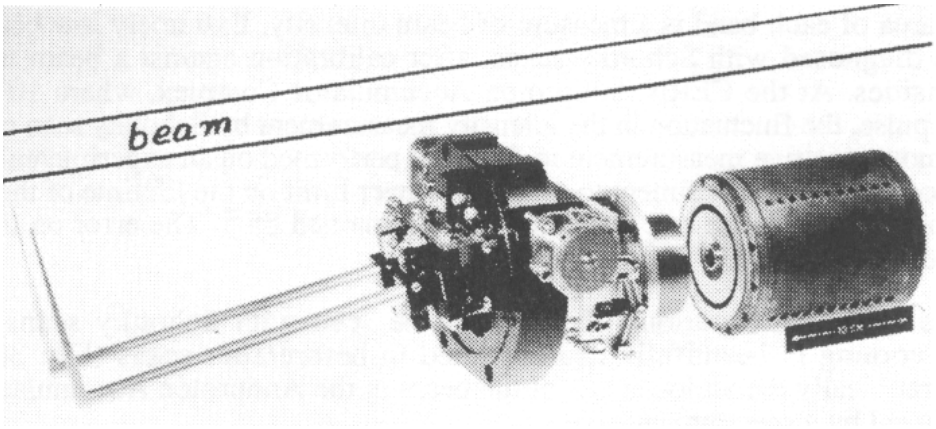

Fig. 27 Fast flip-target. The position of the blades is preadjusted outside the beam.

2.14 Schottky scans

This technical jargon term means scans in frequency, using a spectrum analyzer, of the Schottky signals emanating from a circulating beam. Schottky signals are at the basis of stochastic cooling but their great potential for diagnostic purposes was soon recognised [41]. This subject has become quite vast and here we can only point out some salient features.

Consider a single particle, circulating in a storage ring and observed with an ideal pick-up (PU) of infinite bandwidth. The signal delivered by the PU is a series of delta-function-like spikes, spaced by 1 revolution period t_{rev}, as shown in Fig. 28 a. A spectrum analyzer then displays what is shown in Fig. 28 b: a series of spectral lines, spaced by the revolution frequency f_{rev}.

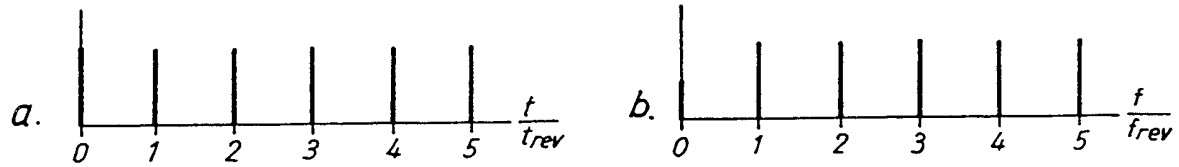

Fig. 28 a) Time domain : signal on a PU from a single circulating particle
b) Frequency domain : corresponding spectrum.

In a beam there are many particles and since there is a spread in their momentum, there will also be a spread in their revolution frequency. The observed Schottky signal can be

regarded as the sum of all individual signals or as the noise stemming from statistical density fluctuations [42]. The spectrum will be as in Fig. 29, with bands instead of lines, their width proportional to h = f/frev and, provided the vertical coordinate is the spectral power density, all of equal area. From such a scan, f_{rev}, Δf_{rev} and (assuming η = [df/f]/[dp/p] is known) Δp are immediately obtained.

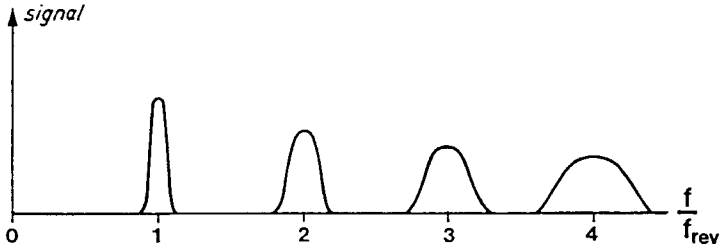

Fig. 29 Schottky scan of a many-particle beam with a spread in momentum and therefore in frequency.

The area of each band is a measure of beam intensity. Extremely low beam intensities can thus be diagnosed with Schottky scans, after calibration against a beam transformer at higher intensities. At the CERN Antiproton Accumulator Complex, where 10^6 to 10^8 π are injected per pulse, the fluctuation in the intensity measurement by Schottky scan corresponds to 10^4 π. The most sensitive measurement to date was performed on an experimental cooling ring, ICE. In the course of an experiment to set a new lower limit on the lifetime of the π, a beam of 250 π was made to circulate and after 86 h there remained 85 π. The error on these numbers was estimated to ± 13 π [43].

Some further illustrations of what can be seen with Schottky scans : Stochastic momentum cooling is beautifully demonstrated in before/after scans (Fig. 30a); Fig. 30b assembles graphically the various parts of the beam in the Antiproton Accumulator as they are indeed displayed by a spectrum analyzer.

Schottky scans are usually made at high harmonics of f_{rev}. Firstly, for a given resolution in Δf_{rev}, the required scan time is proportional to 1/f. Secondly, one often uses the signal from a PU that drives the stochastic cooling. There, a high bandwidth is desired and therefore the PU is more sensitive at high frequencies [44, 45].

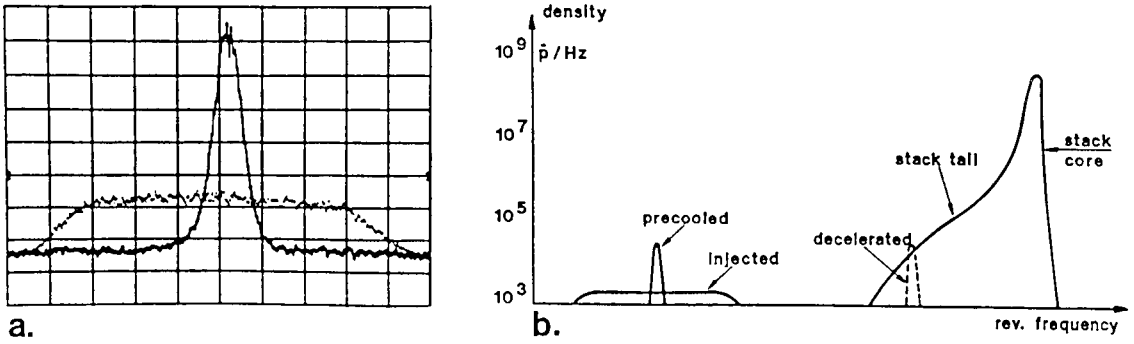

Fig. 30 a) Schottky scans before and after momentum cooling of 6 x 10^6 π in the Antiproton Accumulator. The scan is made around h = 170, at 314 MHz. b) The various parts of the π beam in the same machine, as Schottky scans show them.

A position-sensitive PU will deliver Schottky signals from the betatron oscillations. With a beam centred in the PU and perfect balance and linearity, the harmonics of f_{rev} will not be present. The spectrum (Fig. 31) consists of bands centred at the values

$$f_m = (m \pm Q) f_{rev}$$

where m is the mode number, 0, 1, 2, ...

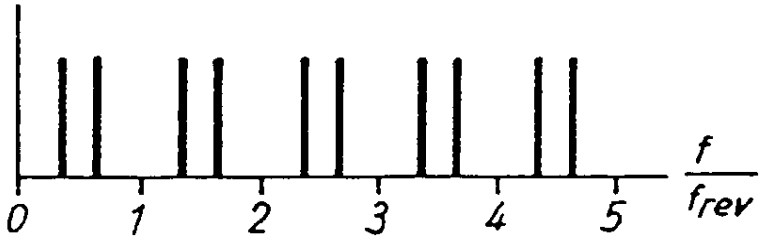

Fig. 31 The signal from a position-sensitive PU contains the frequencies f_m of the "betatron sidebands". Here, the non-integer part of Q is 0.35 or 0.65.

The non-integer part of Q (or its complement to 1, see section 2.17) is thus measured. The width of the bands, together with the knowledge of Δp and the chromaticity of the machine, ξ, yields ΔQ. It is an interesting exercise to show that a particular relation between m, Q, η and ξ, leads to a vanishing width of the band at f_m (Appendix 3).

There exists today an important literature on diagnostics with Schottky signals. To that already quoted we add Ref. [46] and, as the most recent and comprehensive one, Ref. [47].

2.15 Synchrotron radiation

What is a curse for the acceleration of electrons and positrons is a blessing for diagnostics. Synchrotron radiation [48], similar to Schottky noise, is a fairly ideal source of information, it is there for the taking (although the taking may be quite expensive).

Despite the subject's great importance for diagnostics [49, 50], we will be brief here, since it was treated at the same School [51]. Let us just recall two essential features: At practically all electron synchrotrons the spectrum includes the visible range and the light is emitted into a very small angle, roughly E_o/E.

For diagnostic purposes, light is extracted from the accelerator and transported to the measuring equipment by means of various optical elements, such as windows, mirrors, lenses and fibres [52]. The receivers are TV cameras, CCDs, photo diodes (single or in an array), etc. The information drawn may be a simple, but very instructive, TV image on which one can visually follow the evolution of beam size; it may be a precise profile measurement; it may be a bunch length measurement with ps resolution which needs extremely fast oscilloscopes or a streak camera (that's where it gets expensive). Descriptions of such systems are found in Refs. [53, 54, 55]

In the context of synchrotron radiation, because of the dependence on $(E/E_o)^4$, one tends to think only of electrons. However, at the highest energies achieved in the last decade or so, even protons come up against this effect. Not so much yet that it would be a curse, but some blessing is already there. Synchrotron radiation induced by the abrupt change of field at the ends of the bending magnets was detected at the 400 GeV CERN SPS and used for profile measurement [56]. The addition of an undulator [48] provided the necessary enhancement of emission for continuous profile monitoring of the proton and antiproton beams, when the SPS was used as a 270 GeV collider [57].

2.16 LASER Compton scattering

Compton scattering is the exchange of energy between a photon and a moving particle when they encounter each other, as shown in Fig. 32a. The highest gain of energy for the photon will occur in a head-on collision, for which the angle α goes towards zero. A photon of a few eV, in the visible range, encountering a multi-GeV electron or positron, may thus be

propelled to energies of several GeV.

When one shines LASER light onto an electron beam, the resulting high energy γ will accompany the beam until the next bending magnet, where they will fly straight on (Fig. 32 b). By detecting only the γ of highest energies, one selects those which have the same direction as the electron which they had encountered. One can thus measure the density distribution of the electron beam, either by scanning the beam with a fine LASER beam, or by illuminating it fully and evenly.

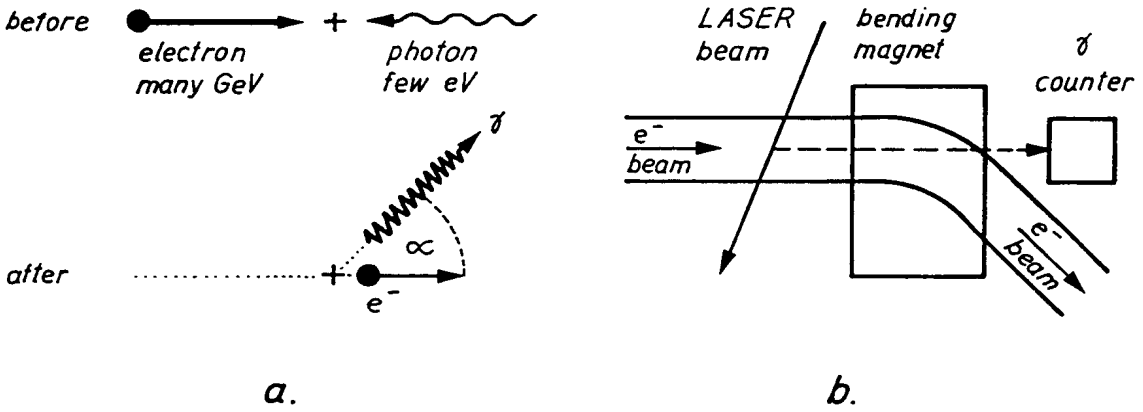

Fig. 32 a) The mechanism of Compton scattering. b) Shining LASER light on an electron beam produces high energy γ, which fly straight on at the next bending magnet.

Compton scattering is used with success for the measurement of electron and positron beam profiles [58, 59, 81]. For proton beams its use is hindered by the fact that the event cross-section is inversely proportional to the rest mass Eo.

2.17 Q-measurement

Q, the number of betatron oscillations per revolution in a circular machine, is really a property of the machine rather than of the beam, although an intense beam, through the forces which its own charge produces, can influence it. The exact value of Q is of great importance in modern machines in which beams may be kept circulating for hours while being subjected to strong non-linear forces, stemming from their own charge or from the second beam in a collider. Sometimes, variations of Q by a few 0.0001 of an integer decide about the well-being of the beam.

A straightforward way to measure Q is to let a bunch of particles perform a coherent oscillation, e.g. by misadjusting injection conditions, and measure the position on all PUs around the ring for one turn. Subtracting from these readings the previously measured closed orbit distortion, normalizing to the square-root of the betatron function at each PU and plotting the result as a function of betatron phase, one obtains a sine-curve, the frequency of which is easily judged to 0.05 of an integer. A merit of this method is that it yields the full value of Q. That is no mean feature, as there have been cases where even the integral part of Q was not as expected (no names shall be mentioned).

A similar method is to deform the closed orbit by means of a single dipolar bump. The change in closed orbit, treated as above, yields a sine-curve with a kink at the location of the bump [60].

Usually, Q is measured by observing the signal from a single PU which, at each revolution, records the position of the beam, excited somehow to perform a betatron oscillation

(Fig. 33).

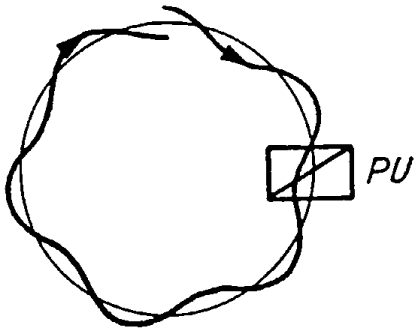

Fig. 33 A single PU records the position of an oscillating beam at every revolution.

As an example, Fig. 34 shows in big dots the position of an oscillating bunch on six subsequent turns. Intuitively, one would draw a sine-curve through the data points and obtain the one labelled 0.23. However, sine-curves of other, higher, frequencies also pass through the same data points. Two, labelled -0.77 and 1.23, are shown, but it is true for all frequencies

$$f_m = (m \pm Q)\, f_{rev}$$

where f_{rev} is the revolution frequency and m the mode. These are the "betatron sidebands" of section 2.14 and Fig. 31.

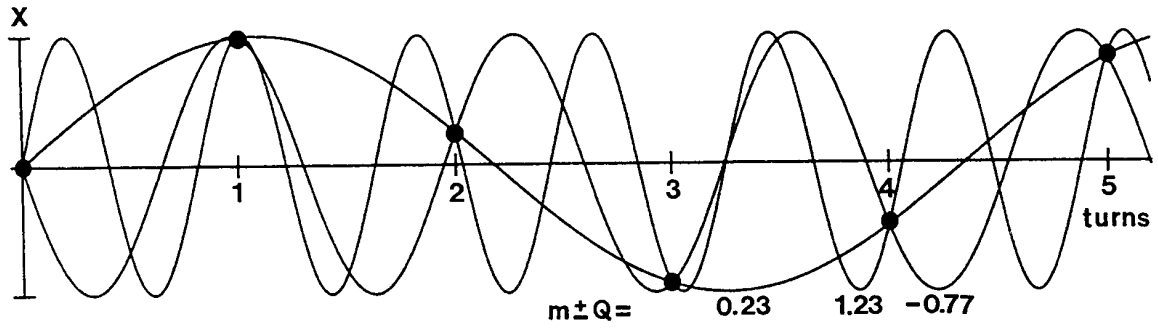

Fig. 34 Beam position on six subsequent turns and the three lowest-frequency fits.

Analysis of the signal from a single PU can deliver very precise results, to a few 0.0001 of an integer, but says nothing about the value of m. As a consequence, not only the integral part, [Q], remains unknown, one can also not distinguish between q = Q-[Q] and its complement 1-q (0.23 and 0.77 in Fig. 34). In order to determine whether q is above or below 0.5, one may change the focusing properties of the machine (e.g. the current in the F and D lenses) and observe in which direction this shifts the frequencies f_m, or one resorts to one of the two first-mentioned methods.

The methods using the signal from a single PU are many. They differ in the way in which the beam is excited and in which the signal is analyzed. Historically, the first method was to excite a beam by applying an rf voltage to a transverse kicker (a pair of electrode plates, Fig. 35a). Scanning with the rf generator, one found the frequencies f_m at which beam loss occurred, hence the term "rf knock-out". Today, one does it more gently, by detecting resonant excitation at harmlessly small amplitudes [61].

Often the beam is excited by a single kick lasting for a fraction of the revolution time [62], (Fig. 35 b). A filter selects a suitable f_m for measurement with a counter, after a delay to allow the filter transients to die away. In selecting the band f_m to be measured, one must

consider length and shape of the kick, since the "response function" depends on them [63]. As can be seen in Fig. 36, it may vanish for certain combinations of parameters, and there will be no signal at the output of the filter.

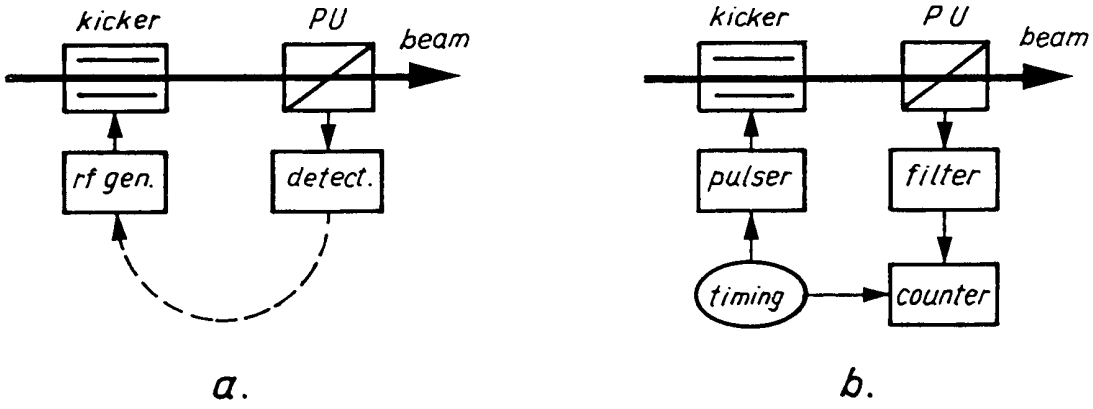

Fig. 35 Q-measurement. a) RF excitation; a feedback loop may provide lock-on. b) Application of a single short kick.

Alternatively, one may digitize the raw signal from the PU and obtain the frequencies f_m through mathematical analysis of the data, usually by Fast Fourier Transform, (FFT).

No excitation at all is needed when one observes the Schottky noise, see section 2.14 and Ref. [47].

Further variants are described in Refs. [61, 64, 65].

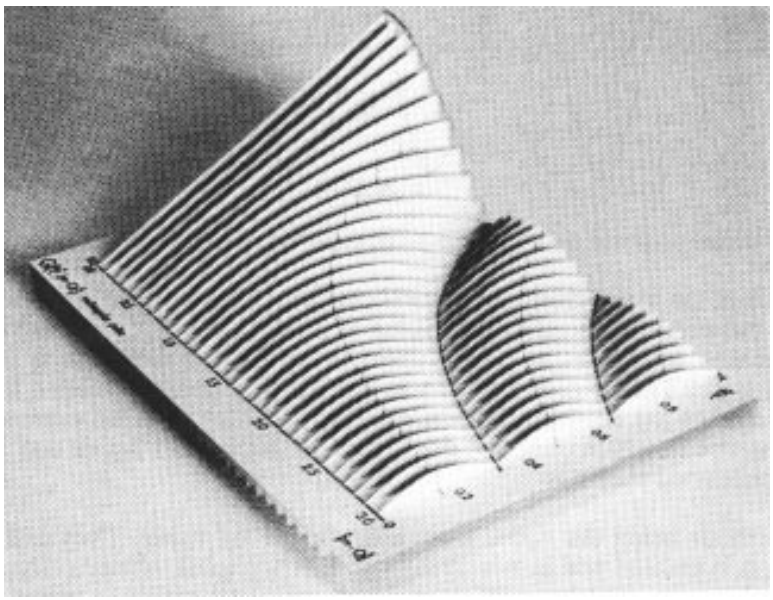

Fig. 36 Response function (vertical axis) for a rectangular kick, as a function of f_m/f_{rev} (left axis) and t_{kick}/t_{rev} (right axis).

2.18 Emittance measurement

Any beam-size measurement on a circulating beam is at the same time an emittance

measurement by virtue of the relation

$$\varepsilon = a^2/\beta$$

where ε is the emittance, a the half-width or -height of the beam and β the value of the beta-function at the place where a is measured. The definition of ε and a is often a source of confusion and needs to be specified clearly.

On beams circulating in storage rings one can observe the betatron bands in the Schottky noise. The area of a band is a measure of the rms betatron amplitude and an emittance can be derived after calibration, e.g. with a scraper, see section 2.13 and Ref. [47].

In transport lines, more than one beam-size measurement is required. For an unambiguous determination of size and orientation of the emittance ellipse, the beam size needs to be known at least at three locations, with known transfer matrices between them and, optimally, a betatron phase advance of 60° [66]. A particularly simple case, as it occurs around a "waist", is shown in Fig. 37. One might think that, because of the symmetry, two measurements would suffice. The third measurement is needed however, to verify that a symmetric situation has indeed been obtained. The most-used device for this purpose is the SEM-grid (see section 2.5).

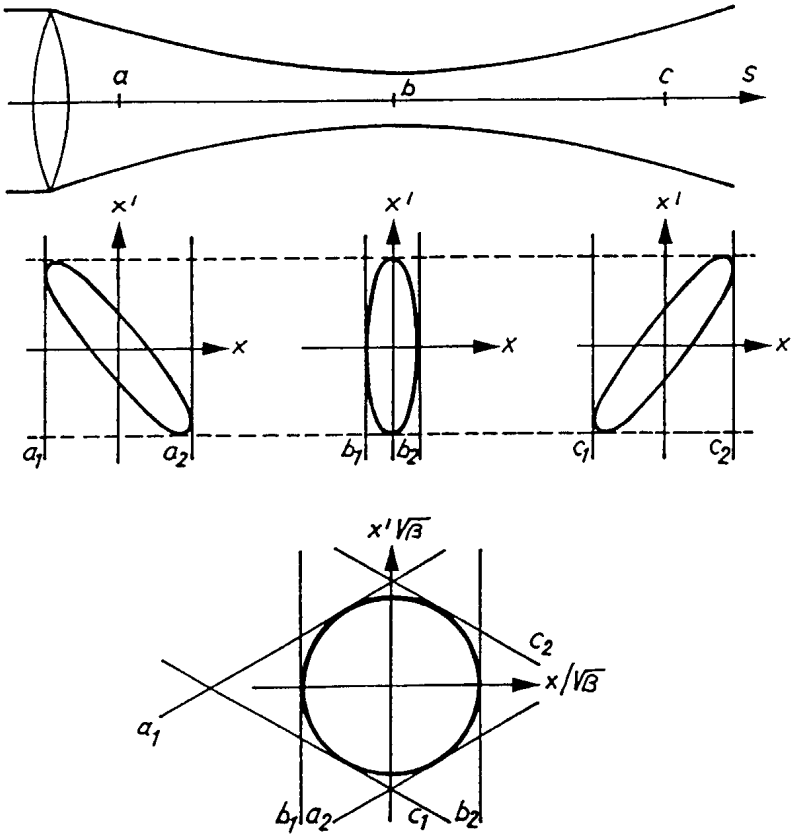

Fig. 37 Emittance ellipses at three locations: at a waist and 60° in betatron phase to either side. Transforming the size-defining lines a_1, a_2, c_1, c_2 to location b, defines the emittance there.

At lower energies, e.g. at the output of a 50 MeV linac, the technique of phase space scanning can be used [67] (Fig. 38).

One arranges for the beam to be fairly wide in the plane in which the emittance is to be measured. A slit selects a narrow slice in x, the transverse coordinate. That slice is left to

diverge over a drift space. Its extension in x' is thus transformed into an extension in x, measured with a profile detector, e.g. a SEM-grid. Scanning the beam over the slit by means of two bending magnets, for every x the extension in x' at the slit is obtained, and the emittance, whatever its shape may be, can be constructed.

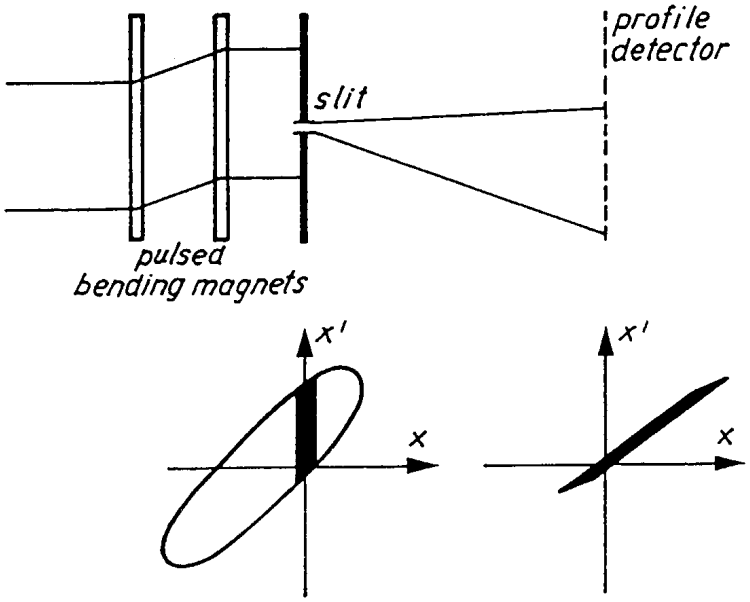

Fig. 38 Phase-space scanning to measure emittance. Above, the basic layout; underneath, the phase-space situation at the slit and at the profile detector.

2.19 Measurement of energy

In a circular machine with well-known orbit length, the energy may be derived from the measurement of revolution frequency, either by counting, when the beam is bunched, or from Schottky scans, when the beam is coasting.

The energy spread, ΔE, of a bunched beam can be inferred from the bunch length, knowing the rf voltage and the factor η (see section 2.14). For coasting beams it is the width, Δf, of a harmonic band, together with η which gives ΔE. All this is basic accelerator physics.

Spectrometers are the evident means to measure the energy and its spread at the output of linacs.

Let us follow the beam as it makes its way through the set-up shown in Fig. 39. The axis of the beam, $x = 0$, shall be the path taken by a particle of central momentum, p_0. To begin with, one produces a wide beam, from which a slit selects a small sample (a). After a drift space, a D-lens greatly increases the divergence of the sample (b) which, after a further drift space, permits an F-lens to rotate the sample such that its width is large and its divergence small (c). This is the situation at the entrance to the bending magnet. At its exit we show three beams : the middle one represents the particles with momentum p_0; the one above those with momentum $p_0 - \Delta p$, more strongly bent; the one below those with momentum $p_0 + \Delta p$, less strongly bent; Δp is shown as the smallest resolved momentum bite. One sees immediately that for good resolution one needs a small sample emittance ε, a large beam width w in the bending magnet and a large angle φ :

$$\Delta p = \frac{\epsilon}{w\varphi}$$

which explains what we have done to the beam so far. The separation in x' of the three

representative beams must now be converted into a separation in x, so that it can be measured. First, an F-lens introduces a strong convergence (e) and after a final drift space the desired separation in x is achieved at a profile detector placed there (f). Overall, one might see this as a highly chromatic imaging of the slit onto the profile detector.

Such spectrometry is relatively easy to perform on 50 MeV protons but becomes difficult with increasing energy. Not only because the magnets will necessarily be bigger, but, more basically, because it becomes impossible to make a slit which, on the one hand, is thick enough to stop the particles outside the wanted sample, and, on the other hand, constitutes a limit only in x and not in x'.

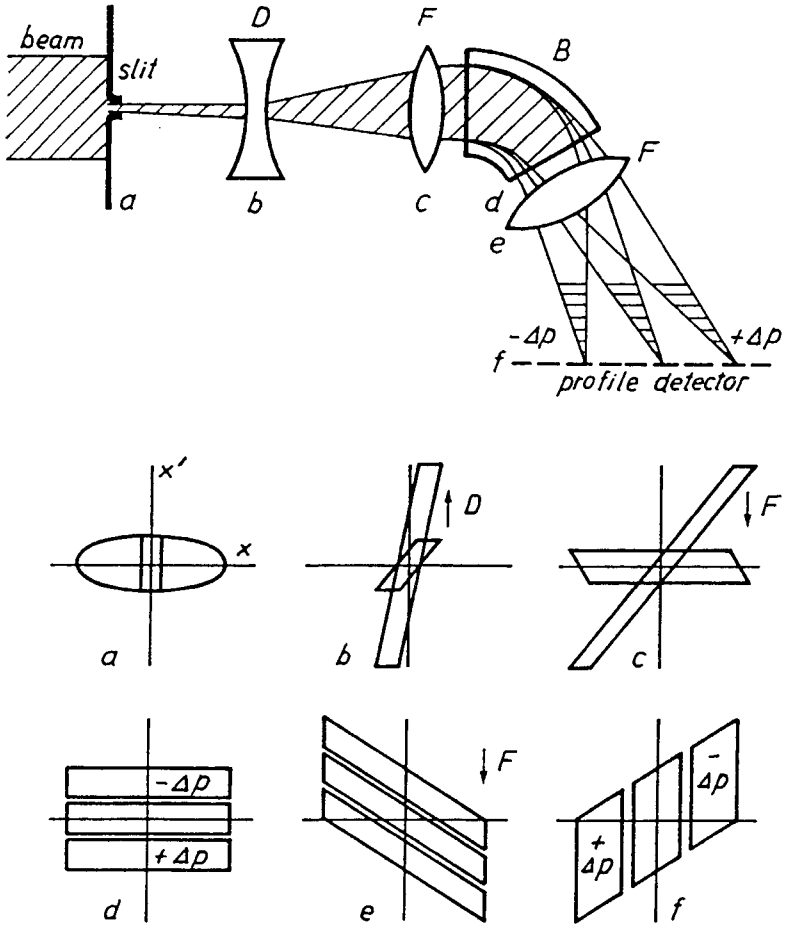

Fig. 39 Above : Basic layout of a spectrometer. D : defocusing lens, F : focusing lens, B : bending magnet. Underneath : the situation in phase space at the six significant locations a - f.

2.20 Polarimetry

Sometimes the experimental physicists delight in polarized beams and the accelerator physicists strive to provide them. A beam is said to be fully polarized, P = 1, when the spin of all particles in it is pointing in the same direction, up or down. A beam is unpolarized, P = O, when the spins of the particles do not have a preferred orientation, half of them will be up, the other half down.

Polarized beams are not easy to produce. Also, polarization may be lost during acceleration, on so-called depolarizing resonances. P is therefore a quantity to be monitored all along, from the source until delivery to the physics experiment. As announced in the

introduction, this is too specialized a subject for an introductory course. We will just mention three kinds of methods and refer to the literature.

Firstly, P can be measured in the physics experiment itself, through the asymmetry in the scattering of the beam particles or in the products of their collisions with target nucleons [68, 69]. This accurate determination can serve as a calibration for other methods.

Secondly, a thin fibre can be brought into the beam, even into the fringe of a circulating beam, and the asymmetry in the scattered particles observed (Mott scattering) [69, 70].

Thirdly, the cross section for Compton scattering depends on the polarization of both the particles and the photons. By shining polarized LASER light onto a circulating beam, P can be determined [58, 71, 72, 73].

3. CONCLUDING REMARKS

I would like to conclude with some advice, first on the technical-operational level.

It is important that calibration, automatic or on demand, can be performed remotely and without interruption to the operation of the accelerator. This applies particularly to beam transformers and position pick-ups.

Status signals must indicate the good order of a device and permit remote fault diagnosis.

Diagnostic systems usually rely for data processing and display of results on a small local computer or are linked to a larger central controls computer. I consider it important that the software, which contains the understanding of the measurement and determines the way in which the desired information is extracted, be conceived, if not written, by the person who has conceived the diagnostic device.

Lastly, and this is true for all components of a machine: good documentation is indispensable for efficient use of the systems and for their maintenance.

In a more general vein, it is no idle advice that before designing the diagnostic equipment for a machine, one should first acquaint oneself with the machine and its possible modes of operation and with the properties and behaviour the beam may show under various conditions. One will take into account not only the "nominal" beam, but also what it might be like in an early stage, the running-in, of the machine and under abnormal conditions, when one is particularly dependent on diagnostics.

One will think of tricky measurements the machine experimenters will want to carry out in order to further performance and basic knowledge, but equally consider the need for precise, unfailing and easily perceived information during routine operation.

Often diagnostic equipment is added on at an advanced state in the design of an accelerator. That is wrong. Diagnostic systems must be included in the design at an early stage, otherwise only too often one finds that no space is left at the best suited locations, or even none at all.

Another important aim, when building a new accelerator, is to have a complete set of diagnostic systems tested and ready for use on the day of first beam. Not only is adequate equipment with diagnostics essential for an efficient running-in of the accelerator, it is also an economic investment in terms of time, pain and simply cost of electricity that it helps to save.

4 . ACKNOWLEDGEMENTS

My thanks go to those students of this course, in Salamanca in 1988 and in Jyväskylä in 1992, who have helped me by pointing out the weak spots, and to Mrs. L. Ghilardi for her patient and careful preparation of this paper.

5 . LITERATURE

Part I : Previous CAS lectures on beam diagnostics.

ANTIPROTONS FOR COLLIDING BEAM FACILITIES
CERN, Geneva, 11-21 October 1983, Yellow Report CERN 84-15

J. Borer and R. Jung, Diagnostics, p.385, vast list of references.

GENERAL ACCELERATOR PHYSICS
Gif-sur-Yvette, Paris, 3-14 September 1984, Yellow Report CERN 85-19

K. Potter, Beam Profiles, p.301
K. Potter, Luminosity Measurements, p.318
P. Wolstenholme, Control Systems of Accelerators, par.6: Beam Instrumentation, p.519

ADVANCED ACCELERATOR PHYSICS
The Queen's College, Oxford, 16-27 September 1985, Yellow Report CERN 87-03

D. Boussard, Schottky Noise and Beam Transfer Function Diagnostics, p.416

SECOND GENERAL ACCELERATOR PHYSICS COURSE
Scanticon Conference Centre, Aarhus, 15-26 September 1986, Yellow Report CERN 87-10

P. Strehl, Beam Diagnostics, p.99
K. Potter, Luminosity Monitoring at LEP, p.153

SECOND ADVANCED ACCELERATOR PHYSICS COURSE
Berlin, 14-25 September 1987, Yellow Report CERN 89-01

D. Boussard, Schottky Noise and Beam Transfer Function Diagnostics

JOINT US-CERN SCHOOL ON PARTICLE ACCELERATORS:
FRONTIERS OF PARTICLE BEAMS, OBSERVATION, DIAGNOSIS AND CORRECTION
Capri, 20-26 October 1988, Lecture Notes in Physics, No. 343, Springer, Heidelberg, 1989.

FOURTH GENERAL ACCELERATOR PHYSICS COURSE
KFA, Jülich, 17-28 September 1990, Yellow Report CERN 91-04

M. Serio, Tune Measurements, p. 136

Part II : References

[1] S. Battisti, CERN/MPS/CO 69-15, 1969.

[2] F. Loyer, T. André, B. Ducoudret, J.P. Rataud, Part. Acc. Conf., Vancouver, 1985. IEEE Trans. Nucl. Sci., NS-32, No. 5.

[3] K. Unser, Part. Acc. Conf., Washington, 1981. IEEE Trans. Nucl. Sci., NS-28, No.3. Also: CERN-ISR-OP/81-14, 1981.

[4] G. Burtin, R.J. Colchester, C. Fischer, J.Y. Hemery, R. Jung, M. Vanden Eynden, J.M. Voillot, 2nd Europ. Part. Acc. Conf., (EPAC 90), Nice, 1990.
Also : CERN/SL/90-30 (BI).

[5] R.T. Avery, A. Faltens, E.C. Hartwig, Part. Acc. Conf., Chicago, 1971. IEEE Trans. Nucl. Sci, NS-18, No. 3. Also : UCRL-20166, 1971.

[6] G. Schneider, IEEE Part. Acc. Conf., Washington, 1987. Also: CERN/PS 87-44 (BT), 1987.

[7] G. Schneider, Thesis, Technical University of Hannover, 1971.

[8] M. Rabany, Part. Acc. Conf., San Francisco, 1973. IEEE Trans. Nucl. Sci., NS-20, No.3. Also: CERN/MPS/Int.BR/73-4, 1973.

[9] G. Gelato, H. Koziol, M. Le Gras, D.J. Williams, Part. Acc. Conf., Washington, 1981. IEEE Trans. Nucl. Sci., NS-28, No.3. Also: CERN/PS/AA/BR/81-19, 1981.

[10] J. Durand, J. Gonzalez, E. Schulte, M. Thivent, 1st European Part. Acc. Conf. (EPAC 88), Rome, 1988. Also: CERN/PS 88-42 (PA), 1988.

[11] G. Nassibian, M. Rabany, CERN/SI/Int.EL/71-2, 1971.

[12] J. Cuperus, Nucl. Instr. Meth., 145, 1977.

[13] T. Katsura, S. Shibata, KEK-79-27, 1979.

[14] J. Borer, C. Bovet, D. Cocq, H. Kropf, A. Manarin, C. Paillard, M. Rabany, G. Vismara, IEEE Part. Accel. Conf., Washington, 1987. Also: CERN/LEP-BI/87-06, 1987.

[15] A. Aragona, C. Biscari, S. De Simone, E. Gianfelice, S. Guiducci, V. Lollo, S. Prella, M. Preger, M. Serio, IEEE Part. Accel. Conf., Washington, 1987.

[16] S. Battisti, M. Le Gras, J.M. Roux, B. Szeless, D.J. Williams, IEEE Part. Acc. Conf., Washington, 1987. Also: CERN/PS 87-37 (BR), 1987.

[17] J.H. Cuperus, Nucl. Instr. Meth., 145, 1977.

[18] W. Barry, CEBAF-PR-89-003, 1989.

[19] J.-C. Denard, G.B. Bowden, G.J. Oxby, J.-L. Pellegrins, M.C. Ross, IEEE Part. Acc. Conf. Washington, 1987. Also : SLAC-PUB-4267, 1987.

[20] R. Bossart, 1st European Part. Acc. Conf. (EPAC 88), Rome, 1988.

[21] Z.D. Farkas, H.A. Hogg, H.L. Martin, A.R. Wilmunder, Proton Lin. Acc. Conf., Chalk River, 1976, Proc.: AECL-5677. Also: SLAC-PUB-1823, 1976.

[22] G. Nassibian, SI/Note EL/70-13, CERN, 1970.

[23] R.H. Miller, J.E. Clendenin, M.B. James, J.C. Sheppard, XIIth Int. Conf. High-En. Acc., FNAL, 1983. Also: SLAC-PUB-3186, 1983.

[24] V. Chohan, F. Pedersen, S. van der Meer, D.J. Williams, 2nd Europ. Part. Acc. Conf. (EPAC 90), Nice, 1990. Also : CERN PS/AR/90-31.

[25] L. Bernard, C. Dutriat, J. Gabardo, M. Le Gras, U. Tallgren, P.Têtu, D.J. Williams, Part. Acc. Conf., Santa Fe, 1983, IEEE Trans. Nucl. Sci., NS-30, No.4. Also: CERN/PS/LEAR/83-15, 1983.

[26] Ch. Steinbach, M. van Rooij, Part. Acc. Conf., Vancouver, 1985. IEEE Trans. Nucl. Sci., NS-32, No.5. Also: CERN/PS 85-33 (OP), 1985.

[27] J. Bosser, J. Camas, L. Evans, G. Ferioli, R. Hopkins, J. Mann, O. Olsen, Nucl. Instr Meth. A235, 1985. Also: CERN SPS/84-11 (DI/MST), 1984.

[28] S. Hancock, M. Martini, M. van Rooij, Ch. Steinbach, Workshop Adv. Beam Instr., KEK, Tsukuba, 1991. Also : CERN/PS/91-12 (OP).

[29] C. Fischer, G. Burtin, R. Colchester, B. Halvarson, R. Jung, J.M. Vouillot, 1st European Part. Acc. Conf. (EPAC 88), Rome, 1988. Also: CERN/LEP-BI/88-12, 1988.

[30] C.W. Fabjan, H.G. Fischer, Reports on Progress in Physics, 43, 1003, The Institute of Physics, 1980.

[31] V. Agoritsas, C. Johnson, CERN-MPS/CO Note 71-51, 1971.

[32] V. Agoritsas, F. Beck, G.P. Benincasa, J.P. Bovigny, Nucl. Instr. Meth., A247, 1986. Also: CERN/PS/85-60 (CO), 1985.

[33] M. Awschalom, H. Howe, R. Shafer, D. Theriot, NAL, TM-274, Batavia, 1970.

[34] B. Vosicki, K. Zankel, Part. Acc. Conf., Washington, 1975. IEEE Trans. Nucl. Sci., NS-22, No.3. Also: CERN-ISR-VA/75-11, 1975.

[35] R. Galiana, D. Manglunki, C. Mazeline, CERN/PS 91-29 (OP), 1991.

[36] C.D. Johnson, L. Thorndahl, Part. Acc. Conf., Washington, 1969. IEEE Trans. Nucl. Sci., NS-16, No.3.

[37] F. Hornstra, DESY HERA 89-04, 1989.

[38] R.W. Allison, R.W. Brokloff, R.L. McLaughlin, R.M. Richter, M. Tekawa, J.R. Woodyard, UCRL-19270, Berkeley, 1969.

[39] S. Yencho, D.R. Walz, Part. Acc. Conf., Vancouver, 1985. IEEE Trans. Nucl. Sci., NS-32, No.5.

[40] H. Schönauer, Workshop Adv. Beam Instr., KEK, Tsukuba, 1991.
Also : CERN/PS 92-10 (HI)

[41] J. Borer, P. Bramham, H.G. Hereward, K. Hübner, W. Schnell, L. Thorndahl, IXth Int. Conf. High En. Acc., SLAC, Stanford, 1974. Also: CERN/ISR-DI/RF/74-23, 1974.

[42] F. Sacherer, CERN-ISR-TH/78-11, 1978.

[43] G. Carron, H. Herr, G. Lebée, H. Koziol, F. Krienen, D. Möhl, G. Petrucci, C. Rubbia, F. Sacherer, B. Sadoulet, G. Stefanini, L. Thorndahl, S. van der Meer, T. Wikberg, Part. Acc. Conf., San Francisco, 1979. IEEE Trans. Nucl. Sci., NS-26, No.3.

[44] S. van der Meer, Nobel Lecture in Physics, 1984. Also: CERN/PS/84-32, 1984.

[45] L. Faltin, Nucl. Instr. Meth., 148, 1978.

[46] D. Boussard, T. Linnecar, W. Scandale, Part. Acc. Conf., Vancouver, 1985. IEEE Trans. Nucl. Sci., NS-32, No.5. Also: CERN SPS/85-30 (ARF), 1985.

[47] S. van der Meer, Joint US-CERN School on Beam Observation, Diagnosis and Correction, Capri, 1988, Proc.: Lecture Notes in Physics No. 343, Springer, Heidelberg, 1989. Also : CERN/PS/88-60 (AR), 1988.

[48] H. Winick, Scientific American, Nov. 1987.

[49] A. Hofmann, Part. Acc. Conf., Washington, 1981. IEEE Trans. Nucl. Sci., NS-28, No.3. Also: CERN-ISR-TH/81-10, 1981.

[50] A. Hofmann, F. Méot, Nucl. Instr. Meth., 203, 1982. Also: CERN/ISR-TH/82-04, 1982.

[51] R. Walker, these proceedings.

[52] M.R. Howells, LBL-20833 Rev., -20834 Rev., -20835 Rev., Berkeley, 1986.

[53] C. Bovet, E. Rossa, Workshop Adv. Beam Instr., KEK, Tsukuba, 1991.
Also : CERN SL/91-18 (BI).

[54] C. Bovet, G. Burtin, R.J. Colchester, B. Halvarsson, R. Jung, S. Levitt, J.M. Vouillot, IEEE Part. Acc. Conf., San Francisco, 1991. Also : CERN SL/91-25 (BI).

[55] S. Battisti, J.F. Bottollier, B. Frammery, E. Marcarini, CERN, PS/LPI/Note 87-13, 1987.

[56] R. Bossart, J. Bosser, L. Burnod, R. Coisson, E. d'Amico, G. Ferioli, J. Mann, F. Méot, Nucl. Instr. Meth., 184, 1981. Also: CERN SPS/80-8 (ABM), 1980.

[57] J. Bosser, L. Burnod, R. Coisson, E. d'Amico, G. Ferioli, J. Mann, F. Méot, Part. Acc. Conf., Santa Fe, 1983. IEEE Trans. Nucl. Sci., NS-30, No.4. Also: CERN SPS/ABM/83-15, 1983.

[58] R. Rossmanith, R. Schmidt, Int. Laser Conf., München, 1981. Also: Internal Report DESY M-81/24, Hamburg, 1981.

[59] K. Wittenburg, DESY-HERA 1986-06, 1986.

[60] M.Q. Barton, R. Frankel, M. Month, Rev. Sci. Instr., Vol.40, No.11, 1969.

[61] I. Farago, K.D. Lohmann, M. Placidi, H. Schmickler, 2nd Europ. Part. Acc. Conf. (EPAC 90), Nice, 1990. Also : CERN/SL/90-40 (BI).

[62] H. Koziol, CERN-MPS/Int. BR/74-14, 1974.

[63] K. Hübner, CERN-ISR-TH/69-17, 1969.

[64] J.P. Potier, G.C. Schneider, E. Schulte, Part. Acc. Conf., San Francisco, 1973. IEEE Trans. Nucl. Sci., NS-20, No.3. Also: CERN/MPS/SR 73-1, 1973.

[65] R. Bossart, A. Chapmann-Hatchett, I. Gjerpe, H.K. Kuhn, T. Linnecar, G. Paillard, C. Saltmarsh, W. Scandale, R. Schmidt, I. Wilkie, Part. Acc. Conf., Vancouver, 1985. IEEE Trans. Nucl. Sci., NS-32, No.5. Also: CERN SPS/85-22 (DI-MST), 1985.

[66] M. Arruat, M. Martini, CERN/PS 92-59 (PA), 1992.

[67] P. Têtu, CERN/PS/LR 79-33, 1979.

[68] T. Khoe, R.L. Kustom, R.L. Martin, E.F. Parker, C.W. Potts, L.G. Ratner, R.E. Timm, Particle Accelerators, Vol.6, 1975.

[69] A.D. Krisch, Journal de Physique, Tome 46, Colloque C2, supplément no.2, 1985.

[70] T. Dorenbos, C.D. Johnson, Conference on High Energy Physics with Polarized Beams and Targets, Argonne, 1976. American Institute of Physics, AIP Conf. Proc. No. 35, Particles and Fields, Subseries No.12, 1976.

[71] R. Schmidt, Workshop Acc. Instr., CEBAF, Newport News, 1991, AIP Conf. Proc., 252, 1992. Also : CERN SL/91-51 (BI).

[72] M. Placidi, R. Rossmanith, Nucl. Instr. Meth., A274, 1989.
Also: CERN/LEP-BI/86-25 Rev., 1988.

[73] D.P. Barber et al., DESY 92-136, 1992.

[74] T. Naito, H. Akiyama, J. Urakawa, T. Shintake, M. Yoshioka, 8th Symp. on Acc. Science and Technology, Wako, Saitama, 1991. Also : KEK Preprint 91-134.

[75] D.A. Goldberg, G.R. Lambertson, US Part. Acc. School , 1991. AIP Conf. Proc., 249, 1992. Also : LBL-31664, 1991.

[76] J. Hinkson, Workshop Acc. Instr., CEBAF, Newport News, 1991, AIP Conf. Proc., 252, 1992. Also : LBL-31526, 1991.

[77] F. Hornstra, 1st Europ. Conf. Part. Acc. (EPAC 88), Rome, 1988.

[78] T. Kawakubo, T. Adachi, E. Kadokura, H. Nakagawa, Y. Ajima, T. Ishida, XIV Int. Conf. High En. Acc., Tsukuba, 1989. Also : KEK Preprint 89-71.

[79] J. M. Schippers, H.H. Kiewiet, J. Zijlsta, Nucl. Instr. Meth., A310, 1991.

[80] C.D. Johnson, CERN/PS/90-42 (AR), 1990.

[81] T. Shintake, H. Hayano, A. Hayakawa, Y. Ozaki, M. Ohashi, K. Yasuda, D. Waltz, S. Wagner, D. Burke, XV Int. Conf. High En. Acc., Hamburg, 1992. Also : KEK Preprint 92-65.

[82] K. Wittenburg, 3rd Europ. Conf. Part. Acc. (EPAC 92), Berlin 1992. Also : DESY HERA 92-12.

[83] J.D. Jackson, Classical Electrodynamics, 2nd ed. J. Wiley & Sons, 1975.

APPENDIX 1

INTERACTION OF BEAM PARTICLES WITH MATTER

Several kinds of detectors rely on the interaction of the beam particles with matter, gaseous or solid. The effects made use of are :

- ionization of gas (residual or molecular jet),
- "secondary emission" of electrons from surfaces,
- production of light (scintillation; in gases, liquids and solids).

All these effects result from the same basic mechanism, transfer of energy through Coulomb-interaction from a beam particle to a shell electron, and therefore exhibit a common functional behaviour.

Consider a beam particle passing close to an atom, at high speed, such that the particle's direction and the "impact parameter" b, i.e. the minimum distance between the particle and the concerned shell electron (see Fig. 40), change little during the encounter.

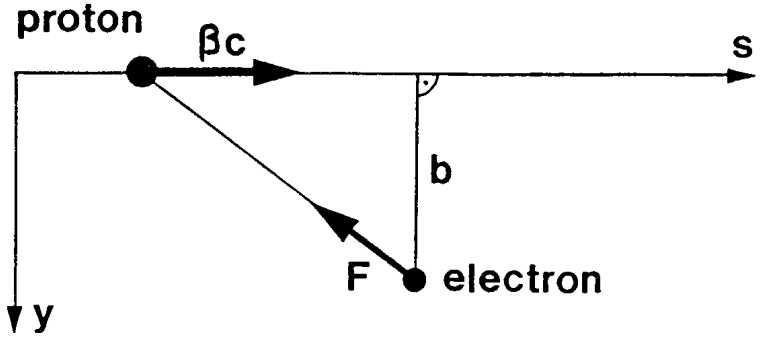

Fig. 40 Encounter between a beam particle and a shell electron. F : Coulomb force, b: impact parameter.

Integrated over the encounter, the longitudinal component, F_s, of the Coulomb force averages to zero, whereas the transverse component, F_y, does not and will impart a transverse momentum, p_y, to the electron :

$$\int_{-\infty}^{+\infty} F_y dt = p_y$$

thus exciting or even ionizing the atom.

From this simple picture we learn the first important fact : electrons are mostly produced at right angles to the direction of the beam (head-on collisions, for which b is very small, with forward-produced electrons, are very rare). The distribution of electron energies extends to very high values, but the bulk of the electrons has energies below 20 eV. On average, a relativistic proton loses some 100 eV per encounter.

In Ref. [83] there is a beautiful derivation of this process and of the Bethe formula, describing the rate at which the beam particle loses its energy. In Gaussian units :

$$\frac{dE}{ds} = 4\pi\ ZN \frac{z^2 e^4}{m\beta^2 c^2}\left[\ln\frac{2m\gamma^2\beta^2c^2}{I} - \beta^2\right]$$

or much simplified $$= \text{const.}\ \rho\frac{z^2}{\beta^2}\ln\left(\frac{p^2}{I}\right)$$

where

N	atoms/cm^3	} of material traversed
Z	atomic number	
I	ionization potential	
ρ	density	
z	charge number	} of beam particle
β,γ	relativistic parameters	
m	electron mass	
e	elementary charge	
c	velocity of light	

This formula shows us the second important fact, namely the dependence on z^2. An ion with charge z will produce z^2 as much light in a scintillator, or as many secondary electrons from a foil, as a proton of the same speed β_c. Seen per charge of the particle, i.e. for the same electrical beam current, the factor is z.

The third important information is the dependence of dE/ds on the particle's energy. Figure 41 shows this in the often used definition of "dE/dx", normalized to the density of the material traversed. For most materials the minimum dE/dx is around 2 MeV/g/cm^2. Characteristic is the sharp increase with decreasing energy (the reason for the so-called "Bragg peak" at the end of the particle's range), which makes low energy particles much more efficient.

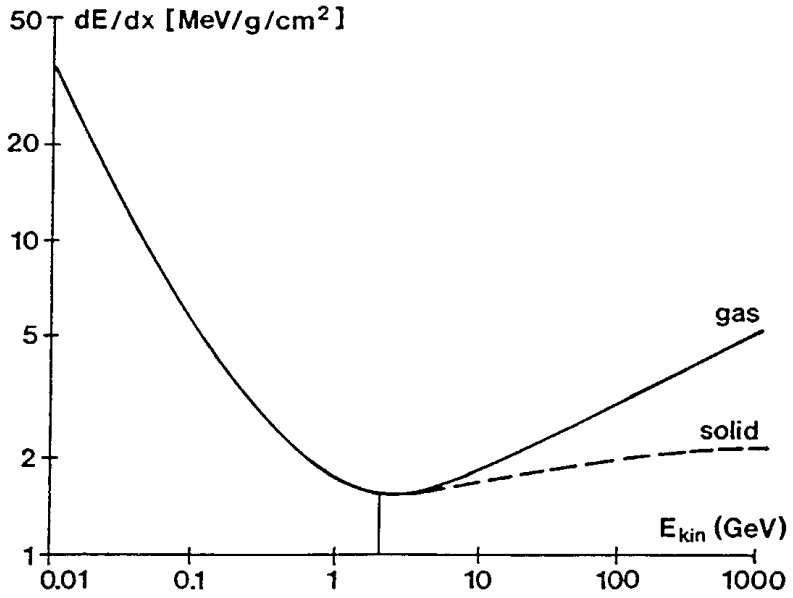

Fig. 41 Typical energy loss of a proton in matter, as a function of kinetic energy.

APPENDIX 2

STATISTICAL LIMIT IN PROFILE MEASUREMENTS

Transverse beam profiles are often measured by collecting electrons or photons, produced by the beam's particles in a gas, from a foil or on a scintillator. The collection occurs into channels, the width of which is given either by the design or by the spatial resolution of the device.

When the beam is very weak, one increases the gain of the amplifiers, with the limit usually seen in the electric noise of the circuits involved. There is, however, a much more basic limitation due to the finite number of electrons or photons collected and the statistical nature of their production.

Let us assume that the projection of the beam's 2-dimensional density distribution onto one plane has a Gaussian shape (Fig. 42), with σ the standard deviation or rms-width.

$$\frac{dn}{dx} = \frac{1}{\sqrt{2\pi}} e^{-\frac{x^2}{2\sigma^2}} \qquad \text{with} \qquad \int_{-\infty}^{+\infty} \frac{dn}{dx}\, dx = 1$$

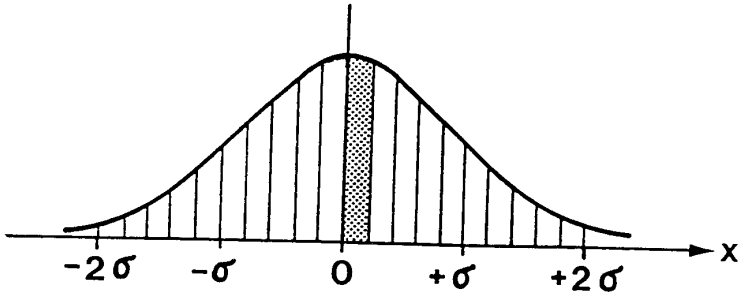

Fig. 42 Distribution of a Gaussian profile over channels 0.2σ wide.

Within a certain time interval, which may be the desired measurement time or simply the time that the beam lasts, the total number of electrons or photons reaching the detector is N_{tot}. Let us take a channel width of $\Delta x = 0.2\sigma$. The 20 channels between $x = -2\sigma$ and $x = +2\sigma$ will collect 0.95 N_{tot} electrons or photons. Consider the central channel, from $x = 0$ to $x = 0.2\sigma$. The number it collects is

$$N_c = 0.083\ N_{tot}$$

The statistical fluctuation on N_c is $\sqrt{N_c}$ and is also called "sampling fluctuation". As an example, let us demand a 5% accuracy on the measurement of central density :

$$\sqrt{N_c}/N_c = 0.05 \qquad \text{therefore} \qquad N_c = 400$$

Since $N_{tot} = N_c/0.083$, we need for a "good" profile measurement at least

$$N_{tot} = 4800 \quad \text{electrons or photons.}$$

Similar exercises can be carried out for other criteria for a "good" profile measurement, resulting in specific compromises between spatial and time resolution.

APPENDIX 3

SCHOTTKY SIDE BANDS OF VANISHING WIDTH

In paragraph 2.14, on Schottky scans, we saw that the spectrum of the signal from a position-sensitive PU contains the frequencies

$$f_m = (m \pm Q) frev \qquad \text{mode number : } m = 0, 1, 2, \ldots \qquad (1)$$

These are not lines but rather bands of a certain width Δf_m, because the beam particles do not all have the same momentum and both f_{rev} and Q depend on momentum. With Δp the momentum spread of the particles :

$$\Delta f_m = \Delta p \frac{df_m}{dp}$$

We mentioned the interesting fact that under certain conditions the width of these bands may shrink to very small values, indeed vanish. This happens when the dependence of f_{rev} and the dependence of Q on momentum (the chromaticity) just cancel each other, so that $df_m/dp = 0$. Differentiating Eq. (1) with respect to momentum p :

$$\frac{df_m}{dp} = (m \pm Q)\frac{df_{rev}}{dp} + f_{rev}\frac{d(m \pm Q)}{dp} \qquad (3)$$

$$= (m \pm Q)\frac{df_{rev}}{dp} \pm f_{rev}\frac{dQ}{dp} \qquad (4)$$

We introduce the chromaticity $$\xi = \frac{dQ}{dp / p} \qquad (5)$$

and the relation $$\eta = \frac{df_{rev} / f_{rev}}{dp / p} \qquad (6)$$

η is a function of energy, $\gamma = E/Eo$, and of the transition energy γ_{tr}, a property of the machine lattice :

$$\eta = \left(\frac{1}{\gamma^2} - \frac{1}{\gamma_{tr}^2}\right) \qquad (7)$$

Inserting Eqs. (5) and (6) into Eq. (4) :

$$\frac{df_m}{dp} = \left[(m \pm Q)\eta \pm \xi\right] \qquad (8)$$

which will be 0 when $$(m \pm Q)\,\eta = \mp\,\xi \qquad (9)$$

or $$(m - Q)\,\eta = \xi. \qquad (10)$$

When condition (10) is fulfilled, the width Δf_m of the betatron band will vanish. Looking for that line in the spectrum and knowing η, one obtains the chromaticity ξ (or vice versa).